People's Democratic Republic of Algeria

Ministry of Higher Education and Scientific Research

University Yahia Fares of Medea

Faculty of Technology

Department of Electrical Engineering



End Master Project

Submitted for the Master's degree

speciality : **Automation and Systems**

PERFORMANCE CONTROL OF HEV POWERTRAIN SYSTEM WITH OPTIMAL BATTERY SIZING CONFIGURATIONS

Realized by :

ARIBI Mohammed El Amin

KHALFAOUI Mohammed Faical

Supervised by :

Dr. KHERKHAR Abdelkrim

Academic year 2024/2025

Acknowledgments

First, we thank ALLAH for giving us strength, patience, and guidance throughout the completion of this work.

We express our sincere gratitude to our thesis supervisor, Dr.KHERKHAR Abdelkrim, for his invaluable guidance, insightful feedback, and unwavering support during every stage of this work.

We also wish to thank the members of the examination jury in advance for accepting to review our thesis and for the time they will devote to evaluating our work.

Our heartfelt thanks go to the Department of Electrical Engineering for the years of rigorous academic formation, which provided us with a solid foundation in our field.

Finally, we gratefully acknowledge Uiversity Yahia Fares of Medea for its ongoing efforts to develop the institution and provide better conditions for study and research.

Dedication – Aribi Mohamed El Amin

This work is dedicated to my parents, who have shown me more than just support: for their unwavering belief in my dreams, their countless sacrifices, and the lessons of resilience and integrity they have instilled in me.

To my two brothers and my new niece, whose presence brings joy and inspiration to our family; and to my extended family and friends, whose encouragement, patience, and kindness have helped me persevere through every challenge.

To all the professors and instructors at the Faculty of Technology, and especially to those who guided us during our specialization in Automatic: for creating a stimulating academic environment, for sharing their expertise, and for their unwavering support and encouragement throughout these years.

To all the students of our class—thank you for the camaraderie, the late-night study sessions, and the collaborative spirit that made every project and exam feel like a shared journey.

A special mention to my dear friends Azzedine, Hassen, Hamza, Sidali, Yacin, and Abdelfattah your friendship, support, and good humor have been a constant source of motivation throughout this journey.

Dedication – KHALFAOUI Mohamed Faical

This work is dedicated to my beloved parents, for their endless sacrifices, constant encouragement, and unconditional love that have shaped who I am today.

To my two brothers and my two sisters, thank you for being my source of strength, for believing in me, and for always standing by my side through every step of this journey.

To my extended family and friends, your support, kindness, and motivation have helped me overcome challenges and stay focused on my goals.

To all the professors and instructors at the Faculty of Technology, especially those who guided us during our specialization in Automatic: thank you for your dedication, for sharing your knowledge, and for helping us grow both academically and personally.

And to all my classmates—thank you for the unforgettable moments, the teamwork, and the spirit of unity that made these years truly meaningful.

To my dear friends Thank you for being a constant source of encouragement, laughter, and unforgettable memories. Whether it was hiking through mountains or navigating challenges in life, your companionship made the journey better. A special mention to: Ismail, Fares, Anas, Youcef, Adel and Amine — your support and shared adventures truly inspired me.

ملخص

تقدّم هذه الرسالة تطوير استراتيجية متقدمة لإدارة الطاقة للمركبات الكهربائية الهجينة باستخدام التحكم التنبؤي النموذجي MPC واستراتيجية تقليل استهلاك الطاقة المعادلة ECMS. يشمل العمل نمذجة وتصميم مركبة كهربائية تعمل بالبطارية BEV، يليه تحليل تأثير التحكم التنبؤي النموذجي واستراتيجية تقليل استهلاك الطاقة المعادلة على استهلاك الوقود وأداء النظام. تم تنفيذ النماذج في بيئة MATLAB/Simulink باستخدام الخرائط الجاهزة لمحرك الاحتراق الداخلي والمحرك الكهربائي. تُظهر النتائج أن التحكم التنبؤي النموذجي واستراتيجية تقليل استهلاك الطاقة المعادلة يعززان كفاءة الطاقة ويقللان من الاستهلاك.

الكلمات المفتاحية: المركبات الكهربائية الهجينة، إدارة الطاقة، MPC، ECMS

Abstract

This thesis presents the development of an advanced energy management strategy for hybrid electric vehicles (HEVs) using Model Predictive Control (MPC) and Equivalent Consumption Minimization Strategy (ECMS). The work includes the modeling and design of a battery electric vehicle (BEV), followed by analyzing the impact of MPC and ECMS on fuel consumption and system performance. The models were implemented using MATLAB/Simulink with pre-built internal combustion engine (ICE) and electric motor (EM) maps. The results show that MPC and ECMS enhance energy efficiency and reduce consumption.

Keywords: Hybrid electric vehicle, energy management, model predictive control, ECMS

Résumé

Ce mémoire présente le développement d'une stratégie avancée de gestion de l'énergie pour les véhicules électriques hybrides (HEV) en utilisant le contrôle prédictif basé sur le modèle (MPC) et la stratégie de minimisation de la consommation équivalente (ECMS). Le travail comprend la modélisation et la conception d'un véhicule électrique à batterie (BEV), suivies de l'analyse de l'impact du MPC et de l'ECMS sur la consommation de carburant et la performance du système. Les modèles ont été implémentés avec MATLAB/Simulink en utilisant des cartes préétablies pour le moteur thermique et le moteur électrique (ME). Les résultats montrent que le MPC et l'ECMS améliorent l'efficacité énergétique et réduisent la consommation.

Mots clés : véhicule électrique hybride, gestion de l'énergie, contrôle prédictif, ECMS

Contents

List of Abbreviations **i**

List of Nomenclature **ii**

General Introduction **1**

Chapter I : Overview of Hybrid Electric Vehicles **3**

I.1 Introduction 3

I.2 Historical Evolution of HEVs 3

I.3 Motivation for Electric Vehicle Adoption 4

I.3.1 Global Growth of Electric Vehicles 4

I.3.2 Environmental and Economic Benefits of EVs 5

I.3.3 Government Policies Supporting EV Adoption 5

I.3.4 EV Adoption Strategies in Developing Countries 6

I.3.5 Key Technologies: Battery and Power Electronics 6

I.4 Categories of Electric Vehicles 7

I.4.1 Main Categories of Electric Vehicles 7

I.4.2 Hybrid Electric Vehicle Configurations 8

I.4.3 Comparative Analysis of EV Types and HEV Architectures 10

I.5 Main Components of Electric Vehicles 12

I.5.1 Electric Motor 12

I.5.2 Battery Pack 12

I.5.3 Power Electronics 12

I.6 Challenges and Outlook for HEVs 13

I.6.1 Technical Challenges 14

I.6.2 Infrastructure and Charging Challenges 14

I.6.3 Economic and Market Barriers 14

I.6.4 Environmental and Policy Considerations 14
I.6.5 Future Outlook 14
I.7 Conclusion 15

Chapter II : Electrical Vehicle Design, Modeling, and Simulation 16
II.1 Introduction 16
II.2 Tesla Model Y Overview 16
II.3 Tesla Model Y Parameters 17
II.4 Modeling and Simulation 17
II.4.1 Simulation Environment and Tools 17
II.4.2 Mathematical Modeling 18
II.4.3 Model Implementation 20
II.5 Simulation Results and Analysis 25
II.5.1 Simulation Setup 25
II.5.2 Battery Block Parameters 27
II.5.3 Simulation Settings and Test Conditions 27
II.5.4 Analysis of Simulation Results 27
II.6 Conclusion 33

Chapter III : Energy Management Using Model Predictive Control in Parallel Hybrid Electric Vehicles 34
III.1 Introduction 34
III.2 Parallel HEV Powertrain Architecture 34
III.3 Hybrid Vehicle Powertrain Model 36
III.3.1 Purpose and Overview 36
III.3.2 Governing Equations 36
III.3.3 QSS Toolbox Implementation 37
III.4 Energy Management Strategy 38
III.4.1 Selection of MPC for Energy Management 39
III.4.2 Control Flow and System Overview 39
III.4.3 MPC Strategy Logic and Workflow 40
III.4.4 MPC Formulation 41
III.4.5 Mode Decision Logic 44

III.5 Simulation Setup 45
III.5.1 Model Initial Conditions and Parameters 45
III.5.2 MPC Settings 45
III.5.3 Drive Cycle 45
III.5.4 Simulink Model Overview 46
III.5.5 Simulink Model Subsystem Block 46
III.6 Simulation Results and Discussion 49
III.6.1 General Results 49
III.6.2 Zoomed-In Analysis (800–1 220 s) 53
III.7 Conclusion 54

Chapter IV : Energy-Management System for a P2-Parallel HEV **55**
IV.1 Introduction 55
IV.2 P2-Parallel HEV Architecture 55
IV.3 Equivalent Consumption Minimization Strategy (ECMS) 56
IV.3.1 Instantaneous Hamiltonian 58
IV.3.2 Offline Determination of the Equivalence Factor 59
IV.4 Simulation Model Overview 59
IV.5 Simulation Results and Discussion 60
IV.5.1 Drive Cycle and Power Distribution 61
IV.5.2 Fuel Consumption and Equivalence Factor Behavior 62
IV.5.3 Fixed vs Adaptive s Comparison No Road Load (0 Drag) 63
IV.5.4 Fixed vs Adaptive s Comparison With Road Load (0.05rad Drag) 65
IV.6 Conclusion 66

General Conclusion **67**

List of Figures

I.1 Timeline of Hybrid and Electric Vehicle Developments 4
I.2 Global EV Sales (2012–2024) [1]. 5
I.3 Main categories of electric vehicles [2]. 8
I.4 Three main HEV configurations: (a) Series, (b) Parallel, and (c) Series-Parallel [3]. 9

II.1 Simulink implementation of the Velocity 20
II.2 Simulink implementation of the electric motor model 22
II.3 Transmission process model 23
II.4 Simulink implementation of Battery pack and Motor Current Control 24
II.5 Simulink implementation of Velocity Controller 24
II.6 Simulink block for calculating system efficiency 25
II.7 System Overview Model 26
II.8 Velocity test results from vehicle model. 28
II.9 Armature Current from DC Motor block 29
II.10 Battery Current. 29
II.11 State of charge. 30
II.12 Battery Power Loss. 30
II.13 Mechanical Power Generated By Motor 31
II.14 Electrical Power Given To Motor. 31
II.15 Efficiency of the Motor. 32
II.16 Velocity For Different Np 32
II.17 Battery Power Loss For Different Np 33

III.1 HEV Parallel Configuration Architecture 35
III.2 QSS Toolbox Library blocks for the hybrid-vehicle. 37
III.3 Structure of the MPC Energy Management Strategy 39

III.4 Flowchart illustrating the Model Predictive Control (MPC) process for energy management in the parallel HEV. 40
III.5 Simulink model of a Parallel HEV. 46
III.6 Drive cycle, vehicle model, and gearbox. 46
III.7 MPC-based control unit. 47
III.8 Internal combustion engine and electric motor. 48
III.9 Battery and fuel tank. 48
III.10 Vehicle Speed Profile Over NEDC Driving Cycle (0–1220s). 49
III.11 Engine and Motor Torque Distribution Throughout Driving Cycle. 50
III.12 Battery State of Charge. 50
III.13 Battery State of Charge with MPC-Controlled Charging Events (0–1220s). . . . 51
III.14 Instantaneous Fuel Consumption (L/100km) Under MPC Strategy. 51
III.15 Operating Modes Timeline 52
III.16 Zoomed Vehicle Speed (800–1220s) Highlighting High-Speed Demand. 53
III.17 Zoomed ICE and EM Torque Split (840–1220s). 53

IV.1 Architecture of the P2-parallel HEV 55
IV.2 Flowchart of the Equivalent Consumption Minimization Strategy (ECMS) for real-time energy management. 57
IV.3 Simulink block diagram of the P2-parallel HEV model. 60
IV.4 WLTC drive cycle profile repeated over three iterations. 61
IV.5 ICE and EM torque profiles over the three WLTC cycle. 62
IV.6 Fuel consumption over the three WLTC cycle. 62
IV.7 Dynamic behavior of the equivalence factor s. 63
IV.8 SOC trajectory for fixed and adaptive s (0 drag case). 64
IV.9 Fuel consumption: adaptive s vs fixed s (0 drag). 64
IV.10 SOC trajectory for fixed and adaptive s (drag = 0.05). 65
IV.11 Fuel consumption: adaptive s vs fixed s (0.05rad Drag). 66

List of Tables

I.1 Technical Comparison: ICE vs. BEV vs. HEV vs. PHEV vs. FCEV [4]. 11
I.2 Comparison of HEV Architectures [4]. 11

II.1 General Specifications of the Tesla Model Y [5]. 16
II.2 Tesla Model Y Parameters [5, 6]. 17
II.3 Tesla Model Y Battery Parameters 27

IV.1 Key Simulation Parameters 56

List of Abbreviations

Abbreviation	Full Form / Meaning
AC	Alternating Current
BEV	Battery Electric Vehicle
BLDC	Brushless DC Motor
BMS	Battery Management System
BYD	Build Your Dreams (Chinese EV Manufacturer)
DC	Direct Current
ECMS	Equivalent Consumption Minimization Strategy
EM	Electric Machine (electric motor/generator)
EV	Electric Vehicle
HEV	Hybrid Electric Vehicle
ICE	Internal Combustion Engine
LFP	Lithium Iron Phosphate (battery chemistry)
LHV	Lower Heating Value (of fuel)
MPC	Model Predictive Control
NEDC	New European Driving Cycle
OBC	On-Board Charger
PHEV	Plug-in Hybrid Electric Vehicle
SoC	State of Charge (battery)
WLTC	Worldwide Harmonized Light-Duty Vehicles Test Cycle

List of Nomenclature

Symbol	Unit	Description
P_{ICE}	W	Power output of the internal combustion engine
T_{ICE}	N m	Torque produced by the internal combustion engine
ω_{ICE}	rad/s	Angular speed of the internal combustion engine
P_{EM}	W	Electrical/mechanical power delivered by the electric machine
T_{EM}	N m	Torque of the electric machine
ω_{EM}	rad/s	Angular speed of the electric machine
Q_{BT}	Ah	Battery charge capacity (in Ampere-hours)
SoC	%	State of Charge of the battery (as a percentage)
m	kg	Vehicle (curb) mass
v	m/s	Vehicle linear velocity
F_{trac}	N	Traction force at the wheels
η_{ICE}	–	Efficiency of the internal combustion engine (fraction)
η_{EM}	–	Efficiency of the electric machine (fraction)
J_{axle}	kg·m^2	Rotational inertia at the drive axle
R_{bt}	Ω	Internal resistance of the battery pack

Symbol	Unit	Description
U_{oc}	V	Open-circuit voltage of the battery
C_{bt}	Ah	Nominal capacity of the battery (in Ampere-hours)
m_{ae}	kg	Equivalent mass for aerodynamic drag
C_d	–	Aerodynamic drag coefficient (dimensionless)
A_{f}	m^2	Frontal area of the vehicle
ρ_{air}	kg/m^3	Air density
μ	–	Rolling resistance coefficient (dimensionless)
g	m/s^2	Gravitational acceleration ($9.81\ \text{m/s}^2$)

General Introduction

In recent years, there has been a growing global concern regarding environmental sustainability, increasing fuel prices, and strict emissions regulations, which have propelled the advancement of more efficient and cleaner transportation systems [7].Hybrid and Electric Vehicles (HEVs and EVs), utilizing electric propulsion either partially or entirely, have surfaced as viable solutions to decrease fuel consumption and minimize greenhouse gas emissions while maintaining performance and driving range [8].

Among these, Battery Electric Vehicles (BEVs) depend exclusively on electric motors that are powered by batteries, providing zero tailpipe emissions and exceptional energy efficiency [9]. Conversely, Hybrid Electric Vehicles (HEVs), which encompass parallel hybrids, integrate an internal combustion engine (ICE) with one or more electric motors (EM) to merge power sources in a versatile and efficient way [10].Effectively managing the energy flow in these systems is essential for attaining optimal performance, efficiency, and sustainability under diverse driving conditions [2].

This thesis examines both Battery Electric Vehicles (BEVs) and Hybrid Electric Vehicles (HEVs) from various viewpoints, encompassing system design, modeling, simulation, and sophisticated energy management techniques [11]. In particular, two contemporary control methods are analyzed: Model Predictive Control (MPC) and Equivalent Consumption Minimization Strategy (ECMS) [12], [13]. MPC establishes a foundation for real-time optimization through predictive modeling, whereas ECMS facilitates an immediate reduction of fuel-equivalent energy usage.

The primary objectives of this thesis are:

1. To provide a comprehensive overview of HEV technologies, configurations,and challanges.

2. To design and simulate a BEV model, analyzing its powertrain performance and dynamics using MATLAB/Simulink.

3. Develop an MPC-based energy management system for hybrid vehicles and evaluate its performance under varying conditions.

4. Implement and compare ECMS as an alternative real-time strategy for energy management, assessing its effectiveness and limitations.

The structure of this thesis is organized as follows:

- Chapter I provides generalities about HEVs, including their architecture, advantages, challenges.
- Chapter II presents the design, modeling, and simulation of a Battery Electric Vehicle (BEV), focusing on powertrain components and performance evaluation.
- Chapter III details the development of a Model Predictive Control (MPC) strategy for energy management in hybrid systems.
- Chapter IV investigates the use of the Equivalent Consumption Minimization Strategy (ECMS) as a control approach and compares it with MPC.

The objective of this thesis is to advance intelligent energy management systems for current electric and hybrid vehicles through the exploration of predictive control and ECMS methods.

Chapter I

Overview of Hybrid Electric Vehicles

I.1 Introduction

The automotive industry is moving further toward electric vehicles as a result of tighter emission standards, growing environmental concerns, and the global movement to use fewer fossil fuels. Hybrid Electric Vehicles (HEVs) are one of these technologies that provides a useful and practical fix.

HEVs combine one or more electric motors with a conventional internal combustion engine (ICE). This combination enhances driving performance, lowers hazardous emissions, and increases fuel efficiency without relying entirely on public charging stations.

An overview of HEVs is given in this chapter. It describes the various hybrid system types, their classification among electric vehicles, their historical background, and the primary factors behind their development. The main related issues are also covered, and an overview of the modeling and simulation work that will be done in the upcoming chapters is provided.

I.2 Historical Evolution of HEVs

The development of hybrid electric vehicles, or HEVs, has been progressing for a while. Robert Anderson created the first electric car in Scotland in 1839. Electric transportation got its start with this.

In 1886, electric taxis were introduced in England. These vehicles were compact and operated using basic electric motors and batteries.

In 1890, Ferdinand Porsche of Austria introduced the Lohner-Porsche Elektromobil, which was recognized as the first hybrid car, combining the capabilities of both an electric motor and a gas engine.

In 1915, the Woods Motor Vehicle Company developed the Dual Power hybrid vehicle, which operated on both electric and gasoline power, with each system functioning independently. This represented an early iteration of the parallel hybrid design.

Due to concerns about pollution and fuel efficiency, automakers began to consider hybrid vehicles more in the 1990s. Audi created a hybrid idea in 1997. Toyota also introduced the Prius in Japan that year. It was the first hybrid to be mass-produced. The Prius was introduced globally, including in the United States, in 2000.

By 2005, additional hybrid models such as the Ford Escape Hybrid were introduced. Toyota and Ford collaborated on hybrid technology to enhance system development. The Prius

remained one of the most favored hybrid vehicles [10].

Companies such as BYD and Tesla have advanced the development of clean and efficient transportation in recent years by introducing fully electric vehicles. With a focus on enhancing battery performance and technology, Tesla in particular has been a leader in electric car technology and has raised the bar for the automotive sector. A summarized timeline of key developments in HEV and EV history is illustrated in Figure I.1.

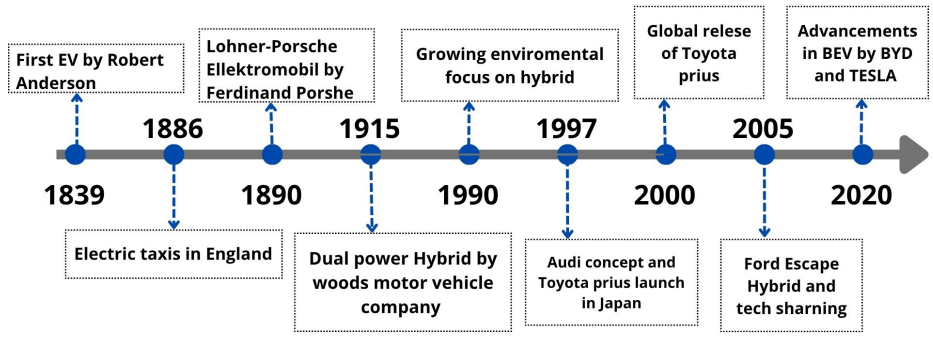


Figure I.1: Timeline of Hybrid and Electric Vehicle Developments

I.3 Motivation for Electric Vehicle Adoption

Advances in technology, supportive regulations, and the pressing need for climate action have made the shift to electric vehicles (EVs) a reality rather than a far away possibility. In this section, the main causes of this change are examined.

I.3.1 Global Growth of Electric Vehicles

Electric vehicle (EV) adoption has surged exponentially over the past decade. In 2022, global EV sales surpassed 10 million units, marking a 55% increase from 2021, with battery electric vehicles (BEVs) dominating 70% of sales [7]. By 2023, sales neared 14 million units, capturing 18% of the global car market—up from 4% in 2020 [1]. China emerged as the global leader, contributing 59% of 2022 sales (4.4 million BEVs and 1.5 million PHEVs), while Europe followed with 2.7 million sales (15% year-on-year growth) [7]. Norway exemplified regional success, achieving 29% EV market share through policies like tax exemptions and toll discounts [7].

Figure I.2. illustrates the continuous growth in global electric vehicle (EV) sales between 2012 and 2024.

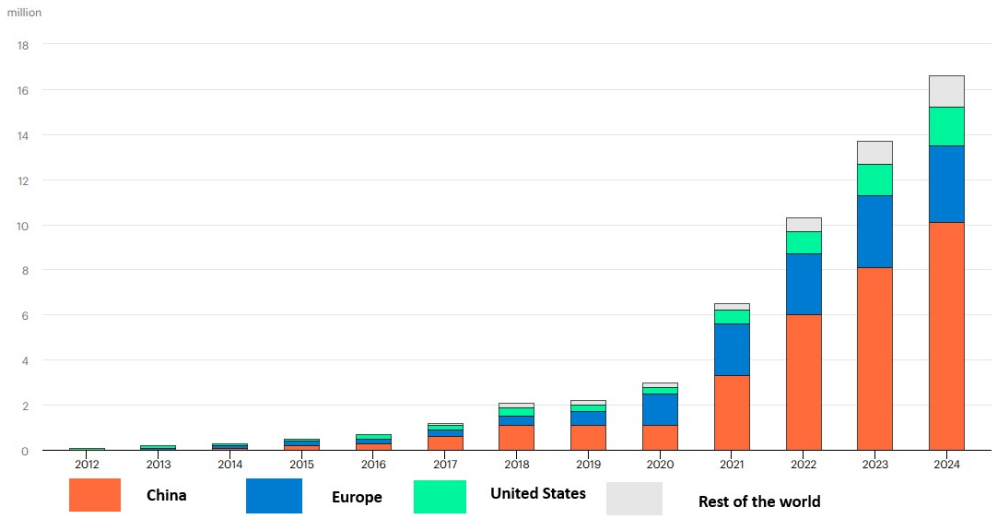


Figure I.2: Global EV Sales (2012–2024) [1].

This rapid adoption reflects broader recognition of EVs' environmental and economic advantages, which we examine next.

I.3.2 Environmental and Economic Benefits of EVs

The transition to EVs addresses two critical global challenges: climate change and energy security. Transportation accounts for 24% of global CO_2 emissions [7], with EVs reducing lifecycle emissions by 50–70% compared to internal combustion engine (ICE) vehicles, depending on regional grid decarbonization efforts [1]. Economically, EVs reduce reliance on volatile fossil fuel markets. By 2030, widespread adoption is projected to displace 6 million barrels of oil daily [1], enhancing energy security for import-dependent nations. Norway's EV adoption, for instance, has already reduced gasoline imports by 15% since 2020 [7].

I.3.3 Government Policies Supporting EV Adoption

Government policies and incentives are pivotal to accelerating EV adoption globally:

- **China**: Dominates global sales through aggressive subsidies, tax exemptions for manufacturers, and Zero-Emission Vehicle (ZEV) mandates requiring automakers to produce EVs [7].

- **Europe**: Norway's 0% VAT on EVs and the EU's 2035 ban on ICE vehicles set benchmarks for policy-driven growth [7].
- **United States**: Federal tax credits under the Inflation Reduction Act (IRA) incentivize domestic manufacturing and consumer purchases, though adoption lags behind China and Europe [7].

I.3.4 EV Adoption Strategies in Developing Countries

Developing nations face unique challenges but deploy tailored solutions to electrify mobility:

- **India**: Struggles with less than 1% 4-wheeler EV adoption due to high upfront costs but sees 4% adoption of electric 2-wheelers, supported by subsidies under the FAME-II (Faster Adoption and Manufacturing of Hybrid and Electric Vehicles) scheme [8].
- **Southeast Asia**:
  - **Indonesia**: Targets 20% EV sales by 2025 through tax reliefs for battery and component manufacturing [14].
  - **Malaysia**: Plans 125,000 charging stations by 2030 under its Low Carbon Mobility Blueprint [14].
  - **Thailand**: Aims to produce 1.2 million EVs annually by 2036, leveraging its automotive supply chain [14].

I.3.5 Key Technologies: Battery and Power Electronics

The rapid evolution of electric vehicles has been enabled by two critical technological advancements: battery systems and power electronics. These components form the foundation of modern EV performance and affordability.

- **Battery Technology Development**

  Battery technology has improved dramatically in recent years. We've seen lithium-ion battery prices drop by 86% from $806/kWh in 2013 to just $115/kWh in 2024 [15]. This huge cost reduction now puts electric vehicles in direct competition with traditional gas cars. At the same time, energy density has jumped to 250 Wh/kg [16], meaning EVs can go much farther on a single charge.Companies like Tesla are pushing things

further too, with designs like their 4680 battery cells that charge faster and last longer [17]. These advancements are key to enhancing EV performance, reducing costs, and supporting broader adoption.

- **Advances in Power Electronics**

  Alongside improvements in battery technology, there have been important advancements in power electronics that are making electric vehicles even better. For example, new technologies like silicon carbide (SiC) inverters and 800V systems are helping to improve the performance, charging speed, and efficiency of electric vehicles.

  - **Silicon Carbide (SiC) Inverters:** SiC inverters have improved EV efficiency significantly. Studies confirm that SiC-based systems reduce inverter losses by exactly 39.8% and overall vehicle energy losses by 6.6% during typical driving cycles. These inverters reach a peak efficiency of 98% and a power density of 70 kW/L, making them smaller and more energy efficient than traditional silicon-based inverters [11].
  - **High Voltage 800V Architectures:** Electric vehicles using 800V architectures benefit from faster charging and better energy handling. Because higher voltage means lower current, there is less heat loss and better cable efficiency. For example, the **Porsche Taycan** charges from 5% to 80% in 22.5 minutes using a 270 kW 800V charger, compared to 90 minutes on a 50 kW 400V charger, using the same connector type [18].

I.4 Categories of Electric Vehicles

Electric vehicles have evolved in a variety of ways in recent years, based on how much they need electric motors and batteries. Understanding the differences among these classifications is crucial to evaluating their effectiveness, cost, and environmental influence. We clearly classify electric vehicles in this part and show the places where hybrid electric vehicles (HEVs) fall into the different types.

I.4.1 Main Categories of Electric Vehicles

Electric vehicles fall into four main groups, each defined by how they get and use power:

- **Battery Electric Vehicles BEVs:** These cars run entirely on batteries, powering electric motors with zero emissions. They are recharged by plugging into the grid.
- **Hybrid Electric Vehicles HEVs:** These vehicles use a combination of an internal combustion engine (ICE) and an electric motor. The battery is charged by the ICE during driving and also through regenerative braking, so there's no need to plug the vehicle in.
- **Plug-in Hybrid Electric Vehicles PHEVs:** Like HEVs, these vehicles combine an internal combustion engine (ICE) and an electric motor, but they have larger batteries that can also be charged by plugging in. This allows them to drive on electric power alone for short distances.
- **Fuel Cell Electric Vehicles FCEVs:** These cars use hydrogen fuel cells to produce electricity, emitting only water vapor. They can refuel quickly, although finding a hydrogen station is still a challenge.

These four types are also shown in a simple way in Figure I.3. which helps make the differences easier to see and compare.

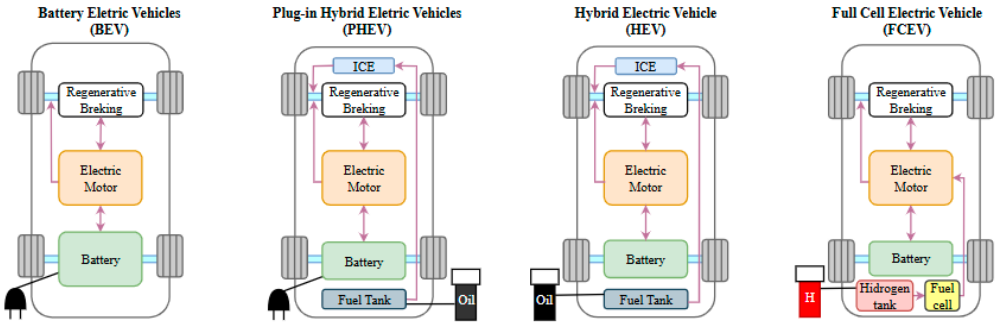


Figure I.3: Main categories of electric vehicles [2].

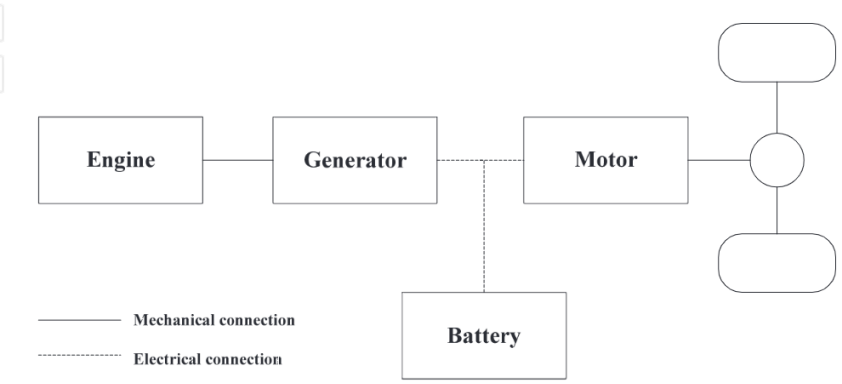
Hybrid electric vehicles (HEVs) combine an internal combustion engine (ICE) with an electric motor to improve fuel efficiency. There are three main configurations of HEVs, each using the engine and motor in different ways. Below, we explain these basic configurations and how they work.

I.4.2 Hybrid Electric Vehicle Configurations

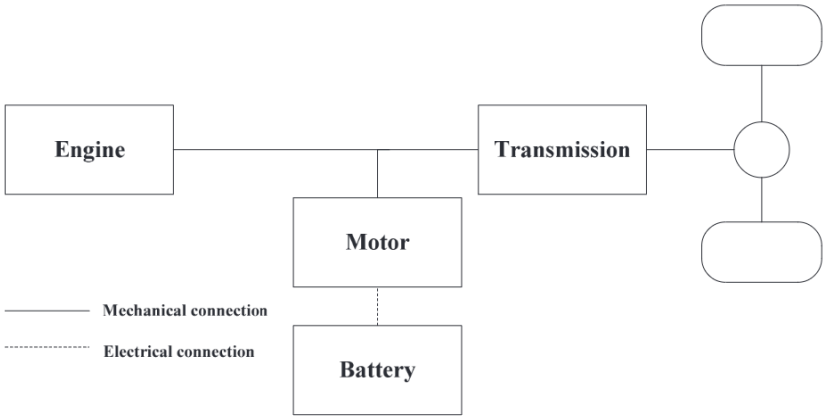
Hybrid electric vehicles (HEVs) are powered by both an electric motor and an internal combustion engine (ICE). Series, parallel, and series-parallel are the three main configurations that

depend on how these parts are connected and function together. Every configuration has an impact on the power delivery and the vehicle's overall efficiency under various conditions.

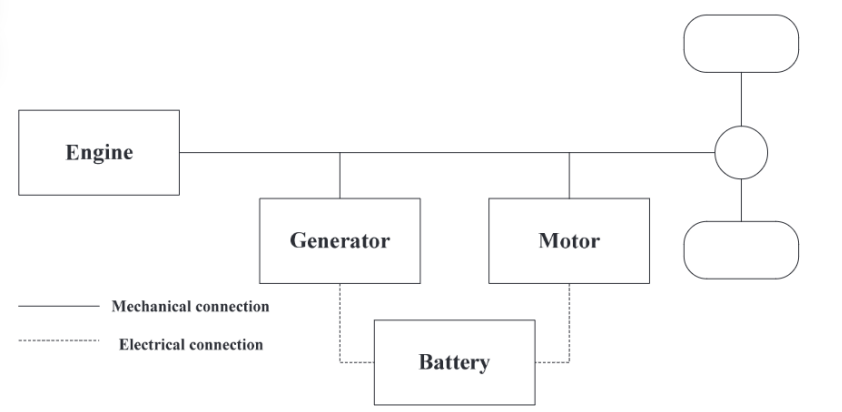
These configurations are also shown in Figure I.4 , which helps make the differences clearer before going into each one.



(a) Series HEV configuration



(b) Parallel HEV configuration



(c) Series-Parallel HEV configuration

Figure I.4: Three main HEV configurations: (a) Series, (b) Parallel, and (c) Series-Parallel [3].

- **Series Configuration:** Only the electric motor powers the wheels in a series hybrid.

Electricity is produced by the internal combustion engine and used to either directly run the motor or charge the battery. Since the engine isn't directly powering the wheels in this configuration, it may operate at its most efficient level.

As shown in Figure I.4a, the ICE is connected to a generator, and the generator powers the electric motor or charges the battery. The electric motor is the only component that moves the wheels.

- **Parallel Configuration :**Both the electric motor and the internal combustion engine are linked to the drivetrain in a parallel hybrid. This implies that the wheels can be powered by one or both of them. Depending on the load, speed, and driving scenarios, the car may combine or alternate between these sources.

  As shown in Figure I.4b , the ICE and the electric motor are connected in parallel to the drivetrain. This allows the vehicle to use the engine for highway driving and the motor for stop-and-go city driving.

- **Series-Parallel Configuration :**Both parallel and series layouts are combined in this type. The vehicle can run on the engine alone, the electric motor alone, or both at once. This configuration adjusts to different driving scenarios, providing flexibility and increased efficiency.

  As shown in Figure I.4c , the system includes components from both series and parallel layouts, allowing for multiple power flow paths depending on the situation.

I.4.3 Comparative Analysis of EV Types and HEV Architectures

Following the presentation of the various hybrid architectures and electric vehicle types, this part offers a comparative overview. The main differences between EV types and HEV configurations are highlighted in the following sections to help you better understand the characteristics and applications.

- **Comparison of EV Types** To provide better context, Table I.1 compares internal combustion engine (ICE) vehicles with various electric vehicle types based on their energy source, charging method, efficiency, and emissions.

Table I.1: Technical Comparison: ICE vs. BEV vs. HEV vs. PHEV vs. FCEV [4].

Feature	**ICE (Gas/Diesel)**	**BEV (Electric)**	**HEV (Hybrid)**	**PHEV (Plug-in Hybrid)**	**FCEV (Hydrogen)**
Main Power	Gasoline or diesel	Battery only	Engine + small battery	Engine + bigger battery	Hydrogen fuel cell
Charging	Fill with gas or diesel	Plug in to charge	No plug – charges itself	Plug in + engine charging	Fill with hydrogen
Emissions	High	None	Low	Low (more if engine used)	None (just water)
Driving Range	300 to 500 miles	100 to 300 miles	Similar to gas cars	20 50 miles electric	Similar to gas cars
Battery Size	None	Big	Small	Medium	Small
Maintenance	High	Low	Medium	Medium	High
Vehicle Cost	Low to medium	Medium to high	Low	Medium	Very high
Efficiency	Low	Very high	Medium	High in electric mode	High

- **Comparison of EV configurations** Table I.2 presents a comparison between different hybrid electric vehicle (HEV) architectures, highlighting their configuration complexity, efficiency, hybridization level, and the control strategy required. This classification helps illustrate how design choices impact both system behavior and integration requirements.

Table I.2: Comparison of HEV Architectures [4].

Architecture	**Configuration Complexity**	**Efficiency**	**Hybridization Level**	**Control Strategy Complexity**
Series	Low	Low	Full HEV, PHEV	Simple
Parallel	Medium	Medium	Micro, Mild, Full HEV	Moderate
Series–Parallel	High	High	Full HEV, PHEV	Advanced

I.5 Main Components of Electric Vehicles

To provide efficient and clean transportation, electric vehicles (EVs) employ a particular combination of components. Understanding these elements helps in clarifying the operation of electric cars (EVs) and their distinctions from traditional internal combustion engine (ICE) vehicles. The main components that are frequently seen in EVs are summarized in this section.

I.5.1 Electric Motor

One essential component of the powertrain of an electric vehicle (EV) is the electric motor. Its main function is to move the wheels by converting electrical energy from the battery pack into mechanical energy. Electric motors used in EVs come in various varieties. These consist of Brushless DC Motors (BLDC), Induction Motors (IM), Permanent Magnet Synchronous Motors (PMSM), and Switched Reluctance Motors (SRM). Every type of motor has unique qualities in terms of cost, performance, and efficiency [19].

I.5.2 Battery Pack

In electric vehicles (EVs), the battery pack serves as the primary energy source. It supplies direct current (DC) electricity to run the car's auxiliary systems and electric motor. Lithium-ion (Li-ion) batteries are used in the majority of EVs today due to their high energy density, extended duration, and quick charging capability [9].

I.5.3 Power Electronics

Power electronics, which regulate the conversion, distribution, and management of electrical energy between multiple components, are essential to the operation of electric vehicles (EVs). The entire performance of the vehicle is maximized by these systems, which provide effective energy transmission between the battery, electric motor, and auxiliary systems.

- **Traction Inverter :** An essential part of electric vehicles (EVs) is the traction inverter, which transforms direct current (DC) from the battery into alternating current (AC) to power the electric motor. Given that the majority of EV motors run on AC, this conversion is essential for effectively driving the motor. The inverter not only provides propulsion but also facilitates regenerative braking, which recharges the battery by reconverting the AC produced by the motor during braking back into DC. In order to increase performance

and energy management, modern inverters are made to function effectively across a broad range of motor speeds and vehicle loads.

- **DC-DC Converter :** By reducing the high-voltage DC from the primary battery to lower voltages appropriate for auxiliary systems like air conditioning, entertainment, and lighting, the DC-DC converter plays a crucial part in EVs. By doing this, possible breakdowns caused on by voltage variations are avoided and all vehicle systems are guaranteed a steady and suitable power supply.

- **Onboard Charger (OBC) :** The role of controlling the flow of electricity from external power sources to the vehicle's battery falls to the onboard charger (OBC). It carries out its essential task of transforming grid-supplied alternating current (AC) into direct current (DC) that the battery can store. The charging speed and energy efficiency of the car are directly impacted by the OBC's efficiency and power rating. Improved onboard charger performance shortens charging times and makes using electric vehicles more convenient and useful overall.

- **Battery Management System (BMS) :** The Battery Management System is vital for keeping a check on and managing the effectiveness, safety, and performance of batteries. It maintains optimal battery health and longevity by monitoring variables as voltage, temperature, and state of charge (SOC). Additionally, the BMS is essential for maintaining battery cell charge balance and guarding against circumstances that can cause battery failure or degradation.

The primary power electronic components found in electric vehicles (EVs) are summarized in this section. In order to ensure effective energy management and vehicle performance, it highlights both their separate roles and their overall impact [20].

I.6 Challenges and Outlook for HEVs

EVs and HEVs are transforming how we travel and move. With their numerous advantages, a number of obstacles continue to prevent their widespread use. These include the absence of enough charging stations, expensive prices, government regulations that are always changing, and technical limitations. The EV business is still developing quickly, though, and many advancements are expected soon.

I.6.1 Technical Challenges

EV battery energy density, typically between 150 and 250 Wh/kg, remains lower than that of liquid fuels, limiting the range of the vehicle and increasing the weight of the pack [16].
Charging an EV can still take between 30 minutes and several hours, while refueling a gasoline vehicle usually takes less than 10 minutes [21].
Battery packs degrade over time, many lose capacity 20% after 1,000 cycles (roughly 200,000 km) [22].

I.6.2 Infrastructure and Charging Challenges

At the end of 2022, there were 2.7 million public charging points worldwide, an increase 55% over 2021, yet deployment remains uneven between urban and rural regions [23].
Electric grids face rising peaks; US EV electricity demand is projected to jump from 24 TWh in 2023 to 468 TWh by 2040, necessitating grid upgrades [24].

I.6.3 Economic and Market Barriers

The average EV sticker price of $72,240 exceeds the $49,988 average for ICE vehicles, deterring cost-sensitive buyers [25].

I.6.4 Environmental and Policy Considerations

Battery manufacturing can emit up to 70 kg CO_2 eq per kWh, raising life-cycle emissions concerns if not offset by clean electricity. [7]

I.6.5 Future Outlook

Solid-state batteries are forecast to enter electric vehicles by around 2026, achieving energy densities near 450 Wh/kg and enabling faster charging and enhanced safety compared to today's lithium-ion cells [26].
Electric vehicles are evolving beyond transportation tools into critical energy infrastructure. The global V2G market is projected to grow 42% annually, skyrocketing from 3.7$ billion in 2023 to 123.6$ billion by 2033 [27].
Smart charging helps reduce electricity peak demand by shifting EV charging to off-peak hours or times of high renewable energy. It can lower peak loads by 6–8% by 2035 [28].

I.7 Conclusion

Hybrid Electric Vehicles (HEVs) were covered in this chapter along with its types, history, development, and essential parts. The causes of the global transition to electric vehicles, including advancements in technology, energy security, and environmental concerns, were also covered.

Modeling and simulation are essential tools for better understanding and enhancing vehicle performance. They enable us to explore energy flows, test powertrain designs, and assess efficiency in various scenarios.

Even though this thesis focuses on HEV systems, the Tesla Model Y, a BEV, opens the following chapter. This decision was made because, before advancing to more advanced HEV setups, BEVs provide a valuable foundation for developing and verifying the simulation model due to their more accessible data and simpler structure.

Chapter II

Electrical Vehicle Design, Modeling, and Simulation

II.1 Introduction

In this chapter, we use MATLAB/Simulink to build and evaluate a computer model of the Tesla Model Y powertrain. We start by going over the vehicle's main specifications and compiling the simulation's required parameters. After that, we create the mathematical models and put them together in a block diagram in Simulink. In order to comprehend energy utilization and performance, we finally execute the simulation and examine the results.

II.2 Tesla Model Y Overview

The rear-wheel drive (RWD) Tesla Model Y is a popular electric car that is recognized for achieving a balance between performance and efficiency. Rear-wheel drive and a lithium-ion battery are its two main components. The table II.1 provides a summary of important features including range, battery capacity, power, and acceleration.

Table II.1: General Specifications of the Tesla Model Y [5].

Specification	**Value**
Real Range	350 km
Vehicle Consumption	164 Wh/km
Battery Capacity (Nominal / Usable)	60.0 kWh / 57.5 kWh
Battery Type	Lithium-ion (LFP)
Voltage (Architecture / Nominal)	400 V / 340 V
Acceleration (0–100 km/h)	6.9 seconds
Top Speed	217 km/h
Total Power	220 kW
Total Torque	420 Nm
Drive Type	Rear-Wheel Drive (RWD)
Fast Charging (10–80%)	25 minutes
Vehicle Mass (Average)	2003 kg

The Tesla Model Y was chosen as the study's reference vehicle because of its regular usage over the world, advanced battery technology, and stable Battery Electric Vehicle (BEV) performance. The model is suitable for testing EV powertrain systems due to its rear-wheel drive

design and economical energy usage. Table II.1 displays the primary technical specifications of Model Y, which provides a general overview before proceeding to the simulation parameters in the next section.

II.3 Tesla Model Y Parameters

The Tesla Model Y powertrain system's main electrical and physical parameters of the Tesla Model Y powertrain system are compiled in the following table II.2. Vehicle dynamics, motor behavior, and battery performance are evaluated using these numbers in force and energy equations.

Table II.2: Tesla Model Y Parameters [5, 6].

Parameter	Value	Description
Vehicle Mass	2003 kg	Balances weight efficiency and structural integrity
Drag Coefficient (Cd)	0.23	Reduces aerodynamic drag, improving efficiency at high speeds
Rolling Resistance Coefficient	0.02	Minimizes frictional losses between tires and road
Air Density	1.29 kg/m^3	Used in aerodynamic drag force calculations
Frontal Area	2.22 m^2	Surface area exposed to airflow, affecting drag
Tire Size	255/44	Affects vehicle traction and efficiency
Wheel Radius	0.38145 m	Influences acceleration and braking performance
Acceleration Due to Gravity	9.8 m/s^2	Standard value used in force and torque calculations
Back EMF Constant	0.245	Determines efficiency of electrical to mechanical energy conversion

II.4 Modeling and Simulation

This section describes the modeling and simulation procedure for the Tesla Model Y. It starts with the tools and simulation environment, then moves on to the mathematical bases, execution, and analysis of the results.

II.4.1 Simulation Environment and Tools

For the simulation, **MATLAB/Simulink**, an effective tool for modeling and simulating dynamic systems, has been used. Battery Electric Vehicles (BEVs) and other complex systems can be built and understood more easily with the Simulink visual block-based interface. The implementation and testing of the Tesla Model Y in this project was made easier by the integrated libraries and toolboxes for electric car modeling.

II.4.2 Mathematical Modeling

The dynamics and performance of an electric vehicle (EV) powertrain can only be effectively simulated by defining a few key equations, especially when dealing with various battery capacity combinations. The electric motor, drivetrain, battery, and power electronics are the main parts of an EV powertrain, and each one is essential to the overall efficiency and behaviour of the vehicle.

II.4.2.1 Battery Modeling

The battery model generally includes equations for the state of charge (SoC), terminal voltage, and internal resistance. In this case, we used the default Lithium-Ion Battery Pack from MATLAB/SIMULINK datasheet, and then adjusted the parameters of the block to match the specifications of the Tesla Model Y's battery pack.

II.4.2.2 Electric Motor Modeling

The electric motor model includes equations for torque, speed, and power:

- **Torque Equation:**

$$T_m = k_t I_m \tag{II.1}$$

  where T_m is the motor torque, k_t is the torque constant, and I_m is the motor current.

- **Current Equation:**

$$V_{in}(t) = L\frac{di(t)}{dt} + Ri(t) + E_b \tag{II.2}$$

$$i(t) = \frac{1}{L}\int (V_{in}(t) - Ri(t) - E_b)dt \tag{II.3}$$

  where R is the resistance, L is the inductance, and E_b is the back EMF.

- **Power Equation:**

$$P_m = T_m \omega_m \tag{II.4}$$

  where P_m is the mechanical power, and ω_m is the motor speed.

II.4.2.3 Power Electronics Modeling

The power electronics, typically an inverter, convert DC power from the battery to AC power for the motor.

- **Inverter Efficiency:**

$$\eta_{inv} = \frac{P_{out}}{P_{in}} \tag{II.5}$$

where P_{out} is the output power, and P_{in} is the input power.

II.4.2.4 Drivetrain Modeling

The drivetrain transmits the motor torque to the wheels and includes losses due to friction and other factors.

- **Drivetrain Efficiency:**

$$\eta_{drivetrain} = \frac{\tau_w \omega_w}{\tau_m \omega_m} \tag{II.6}$$

where τ_w and τ_m are the torques at the wheels and motor, and ω_w and ω_m are their respective angular speeds.

II.4.2.5 Vehicle Dynamics

The vehicle dynamics include equations for acceleration and velocity. Using Newton's second law:

$$m\frac{dv}{dt} = F_{net} \tag{II.7}$$

where m is the vehicle mass and F_{net} is the total force acting on the vehicle.

$$F_{net} = F_{drag} + F_{rr} + F_{grade} \tag{II.8}$$

where the forces are defined as:

- Aerodynamic drag force:

$$F_{drag} = \frac{1}{2}\rho A C_d v^2 \tag{II.9}$$

- Rolling resistance force:

$$F_{rr} = C_{rr} mg \tag{II.10}$$

- Gradient force:

$$F_{grade} = mg\sin(\theta) \tag{II.11}$$

where ρ is air density, A is frontal area, C_d is drag coefficient, C_{rr} is the rolling resistance coefficient, g is gravitational acceleration and θ is the angle of incline.

II.4.3 Model Implementation

This section defines the essential structure of the model. Moving further, we assemble the subsystems in Simulink as the first implementation step. Creating a functional model from the theory and executing initial tests to ensure that everything functions as planned are the tasks of this phase.

II.4.3.1 Vehicle Model

from equations (II.7) to (II.11),we get the expression of the vehicle velocity over time.

$$v(t) = \frac{1}{m}\int \left(F - mg\sin(\theta) - mg \cdot C_{rr}\cos(\theta) - \frac{1}{2}\rho v^2(t) A C_D \right) dt \tag{II.12}$$

The corresponding Simulink model based on this equation is shown in Figure II.1

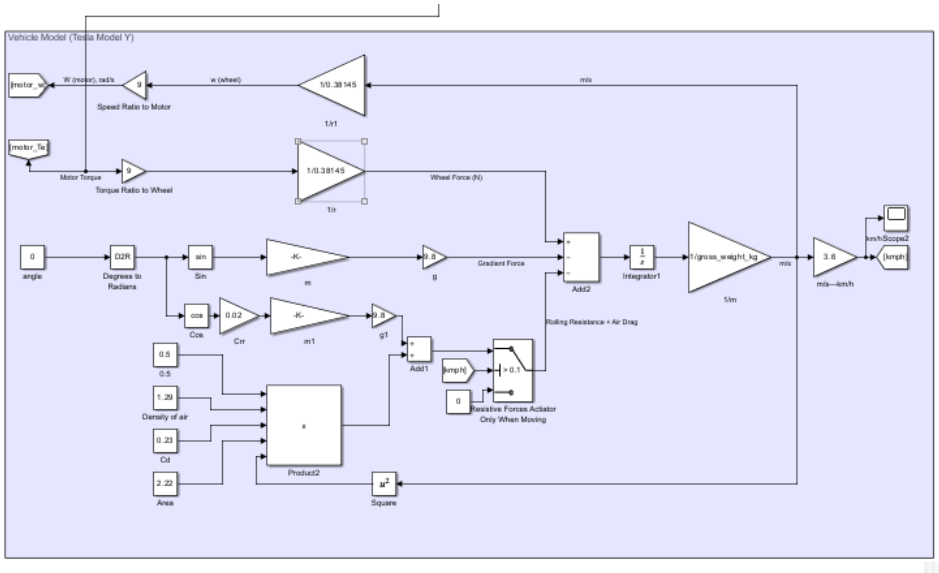


Figure II.1: Simulink implementation of the Velocity

II.4.3.2 Equivalent DC Motor Model

The derived equation for motor current is:

$$i(t) = \frac{1}{L} \int (v_{in}(t) - R \cdot i(t) - E_b)\, dt \tag{II.13}$$

The back electromotive force (EMF) E_b is given by:

$$E_b = K_{bemf} \cdot \omega \tag{II.14}$$

where K_{bemf} is the back EMF constant and ω is the angular velocity of the motor.

The constant power of the Tesla Model Y is approximately 110 kW. Given the battery voltage of 400 V, the estimated current is:

$$I = \frac{P}{V} = \frac{110000}{400} = 275A \tag{II.15}$$

At the top speed of 217 km/h, the total driving force is calculated as:

$$\tau = F \cdot r = 1589.204N \times 0.38145m = 606.2Nm \tag{II.16}$$

This value represents the wheel torque. Assuming a gear ratio of 9:1, the motor torque becomes:

$$\tau_m = \frac{606.2}{9} = 67.35Nm \tag{II.17}$$

Using the torque equation:

$$\tau_m = k_T \cdot I \tag{II.18}$$

we can calculate the torque constant k_T as:

$$k_T = \frac{67.35}{275} \approx 0.245 \tag{II.19}$$

Interestingly, the torque constant k_T and the back EMF constant k_{bemf} are generally equal in many motors. This relationship reflects the law of conservation of energy, where the electrical power input equals the mechanical power output plus electrical losses.

- Back-Calculation of Motor Resistance R At a speed of 60.28 m/s (equivalent to 217

km/h), with a total force $F = 1589.204\,N$, the mechanical power output is:

$$P = F \cdot v = 1589.204 \times 60.28 = 95.8\,kW \tag{II.20}$$

The power loss is calculated as:

$$\text{Loss} = 110 - 95.8 = 14.2\,kW \tag{II.21}$$

Using this, the motor resistance R is:

$$R = \frac{\text{Loss}}{I^2} = \frac{14\,200}{275^2} \approx 0.187\,\Omega \tag{II.22}$$

- inductance The value of inductance L is assumed based on real-life DC motor characteristics. A higher value is used to improve simulation stability:

$$L = 187 \times 10^{-4}\,H \tag{II.23}$$

All these equations and parameters are implemented in the motor model, as shown in Figure II.2. This figure illustrates the detailed Simulink representation used to simulate the motor behavior based on the derived expressions.

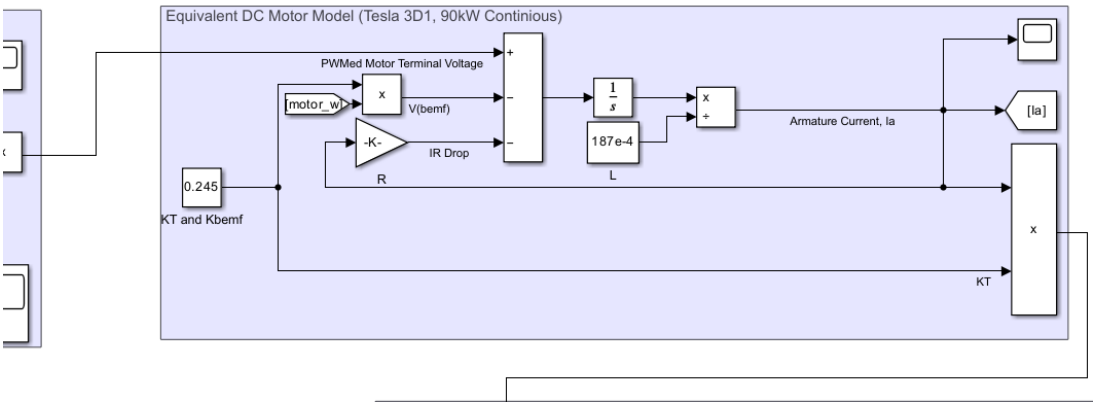


Figure II.2: Simulink implementation of the electric motor model

II.4.3.3 Transmmision Model

There are two transmission processes:

- The first one is from motor torque to wheel force:

$$\text{Wheel Force} = \frac{\text{Motor Torque}}{\text{Gear Ratio} \cdot \text{Wheel Radius}}$$

- The second one is from velocity to angular velocity of the motor:

$$\text{Angular Velocity of Motor} = \frac{\text{Velocity}}{\text{Gear Ratio} \cdot \text{Wheel Radius}}$$

Where Gear ratio = 1:9 and Wheel Radius = 0.38145 m

The transmission processes, which include the conversion from motor torque to wheel force and from velocity to angular velocity of the motor, are illustrated in Figure II.3.

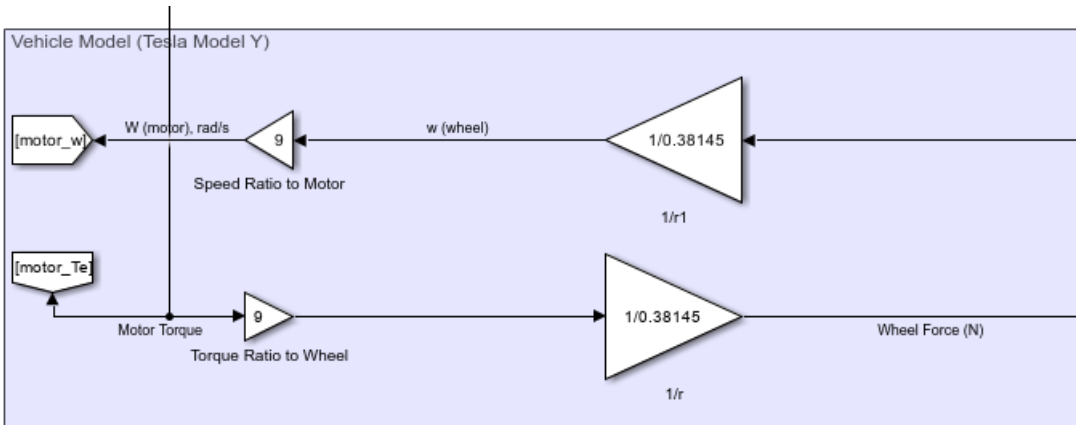


Figure II.3: Transmission process model

II.4.3.4 Battery pack and Motor Current Control

- We used default Datasheet Battery (Lithium Ion) Pack from Matlab and updated the parameters of the block as Tesla Model Y's Battery Pack.
- PWM generator block is used for motor control.
- PI controller is used to control current with feedback.

These components are integrated and illustrated in the Figure II.4.

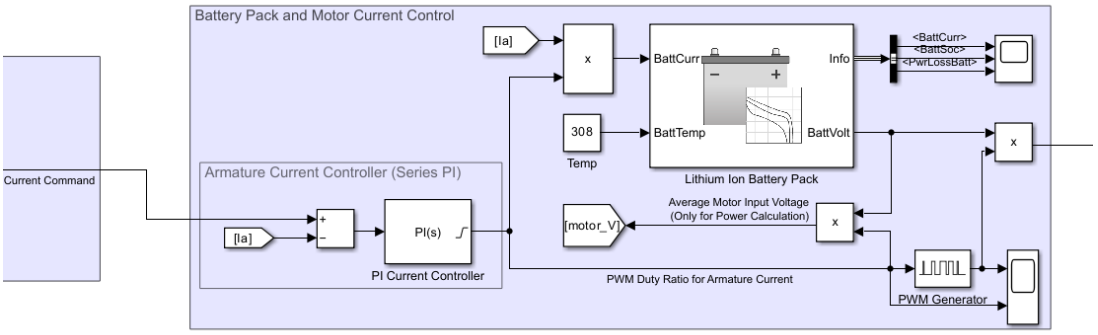


Figure II.4: Simulink implementation of Battery pack and Motor Current Control

II.4.3.5 Velocity Controller

- The velocity controller regulates the motor torque by comparing the desired and actual vehicle velocity, typically using a Proportional-Integral-Derivative (PID) controller.
- Upper and lower saturation limits are applied to constrain the current command sent to the current controller, ensuring safe and stable operation.

The overall control strategy, including the velocity PID controller and current limitation mechanism, is illustrated in the Figure II.5

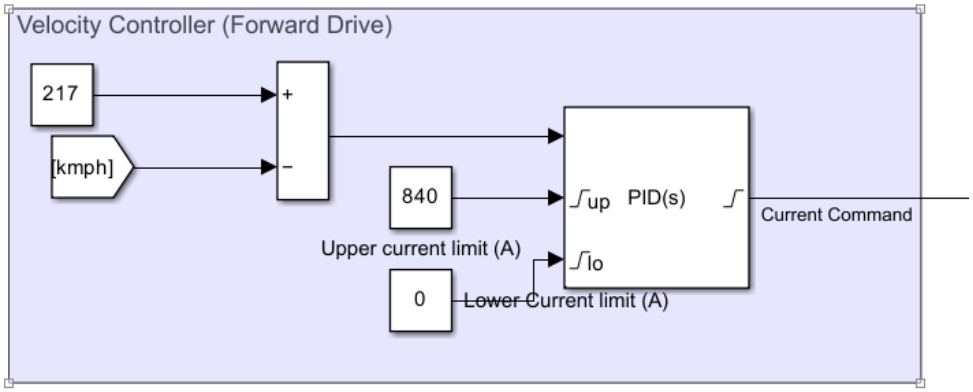


Figure II.5: Simulink implementation of Velocity Controller

II.4.3.6 Power and Efficiency Calculation

Power is calculated for both the mechanical power generated by the motor and the electrical power supplied to it. The efficiency of the system is calculated using the following equation:

$$\text{Efficiency} = \frac{\textit{Mechanical Power generated by motor (kW)}}{\textit{Electrical Power Given to Motor (kW)}} \times 100\% \qquad \text{(II.24)}$$

This efficiency computation is implemented in the Simulink model, as illustrated in the Figure II.6.

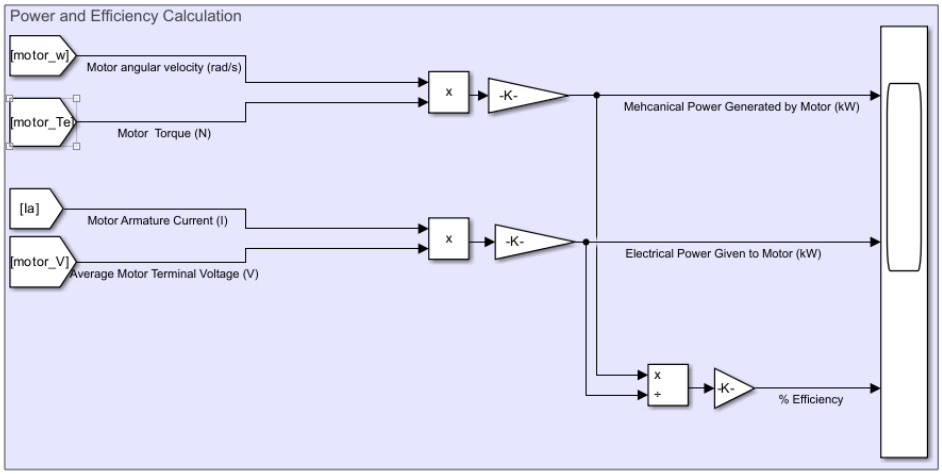


Figure II.6: Simulink block for calculating system efficiency

II.5 Simulation Results and Analysis

This section presents the modeling and simulation results for the Tesla Model Y using MATLAB/Simulink. The complete system is modeled by integrating vehicle dynamics, motor behavior, transmission, battery pack, and control strategies. The goal is to evaluate vehicle performance metrics such as speed, power consumption, and efficiency. The simulation begins with system initialization and parameter definition, followed by execution and result analysis. The first step focuses on configuring the simulation environment, as described in the following subsection.

II.5.1 Simulation Setup

MATLAB/Simulink was used to create the Tesla Model Y simulation by integrating several important components. Each block functions in a closed-loop simulation environment and represents a significant component of the electric vehicle's powertrain:

1. **Vehicle Dynamics:** This block calculates the velocity and acceleration of the vehicle based on the total forces that act on it, such as motor traction, aerodynamic drag, and rolling resistance.

2. **Motor Model:** Simulates the electric motor using equations for torque, speed, and current, considering both electrical and mechanical characteristics.

3. **Transmission:** Converts the motor's torque and speed to the wheels, based on gear ratio and transmission efficiency.

4. **Battery Pack and Current Control:** Models the battery's voltage, internal resistance, and state of charge (SoC). It also includes a current controller that adjusts the motor input to meet torque demands.

5. **Velocity Controller:** A PID controller is used to maintain the vehicle's speed by adjusting the motor torque according to the error between the actual and desired velocity.

6. **Power and Efficiency Calculation:** Calculates the power used and generated in the system, and determines the overall efficiency of the powertrain.

These subsystems are linked in Simulink to form a complete EV model. The integrated system is shown in Figure II.7.

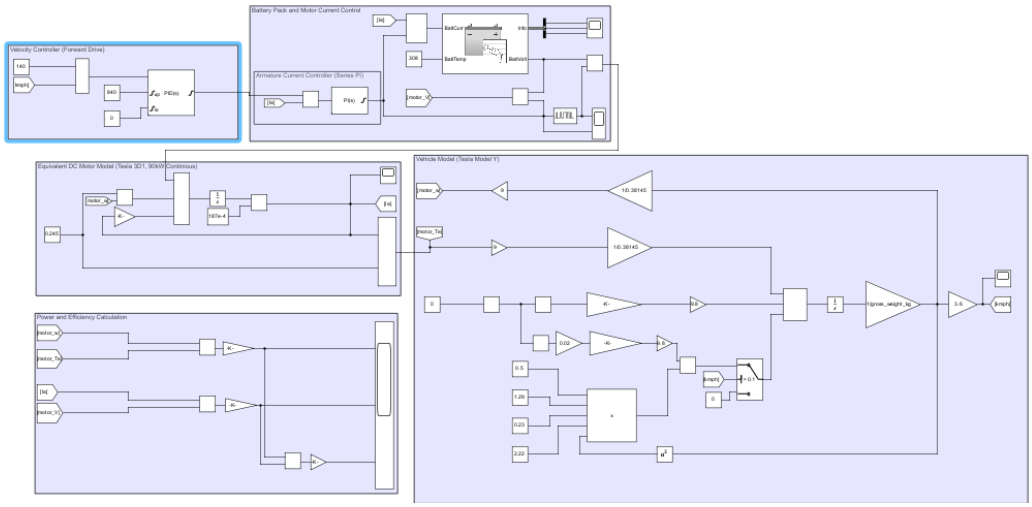


Figure II.7: System Overview Model

The Tesla Model Y BEV model is evaluated under a full acceleration test to assess system performance. The main inputs include a full throttle command, motor torque request, and initial battery SOC. Key vehicle parameters such as mass, drag coefficient, and gear ratio are defined as fixed values. The model outputs include vehicle speed, SOC, battery power loss, armature current, motor power, and efficiency, enabling analysis of energy flow during high-load operation.

II.5.2 Battery Block Parameters

Before running the Simulink model, the battery parameters illustrated in Table II.3 ,must be inserted into the Default Datasheet Battery (Lithium Ion) block.

Table II.3: Tesla Model Y Battery Parameters

Parameter	Value
Battery Voltage	400 V
Cell Capacity	4.8 Ah
Battery Cell Type	2170
Total Battery Cells	4416
Series Configuration	96 cells
Parallel Configuration	46 cells
Total Battery Weight	771 kg
Weight per Series Group	16.7609 kg

II.5.3 Simulation Settings and Test Conditions

The simulation was carried out in MATLAB/Simulink with a total runtime of 120 seconds. The process followed these main steps:

- **Initialize the Simulation:** The Simulink model was checked to ensure that all subsystems were properly connected and parameterized. The simulation duration was set to 120 seconds.
- **Run the Simulation:** The simulation was executed, and its progress was monitored to confirm that it ran without errors or instability.
- **Log Output Data:** Key outputs such as vehicle speed, motor torque, battery voltage, battery current, and powertrain efficiency were recorded for analysis.

II.5.4 Analysis of Simulation Results

The performance data that was obtained after the Tesla Model Y simulation model was successfully run is shown in the following figures. In order to assess the vehicle's dynamic behavior,

energy usage, and overall system efficiency during the simulated driving cycle, these results are examined below.

II.5.4.1 Velocity

The vehicle velocity profile is presented below to evaluate the speed response of the system during the full acceleration .

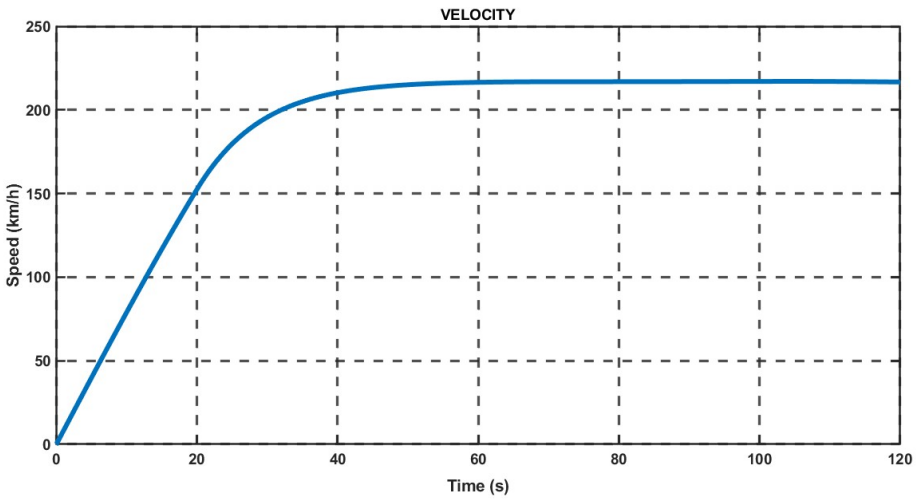


Figure II.8: Velocity test results from vehicle model.

Vehicle Speed quickly accelerates, achieving 217 km/h at 60 seconds and maintaining stability, indicating strong initial acceleration and efficient high-speed cruising capability.

II.5.4.2 Armature Current

The following figure illustrates the armature current drawn by the electric motor, which reflects the motor's dynamic response.

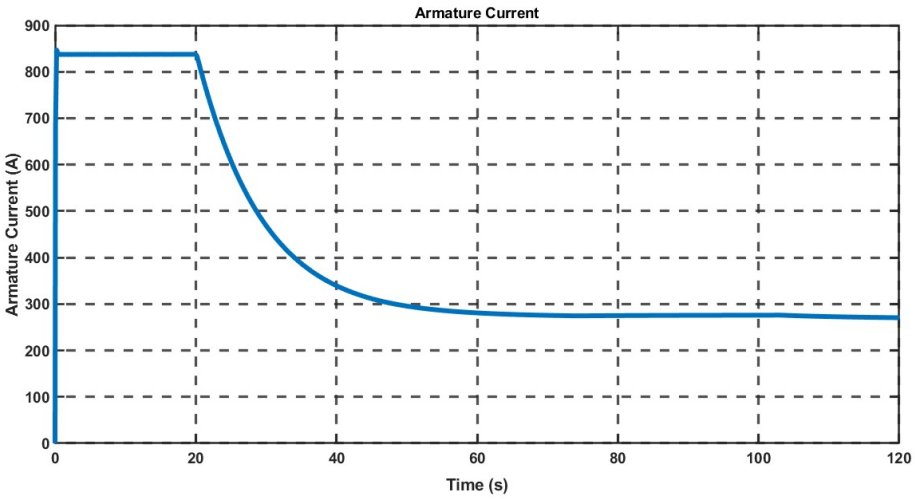


Figure II.9: Armature Current from DC Motor block .

Armature Current starts high 840 A, dropping after acceleration and stabilizing within 300 A, showing initial high torque demand transitioning to lower steady-state requirements.

II.5.4.3 Battery Characteristics

The battery current variation is shown below, indicating the energy flow between the battery and the rest of the powertrain during operation.

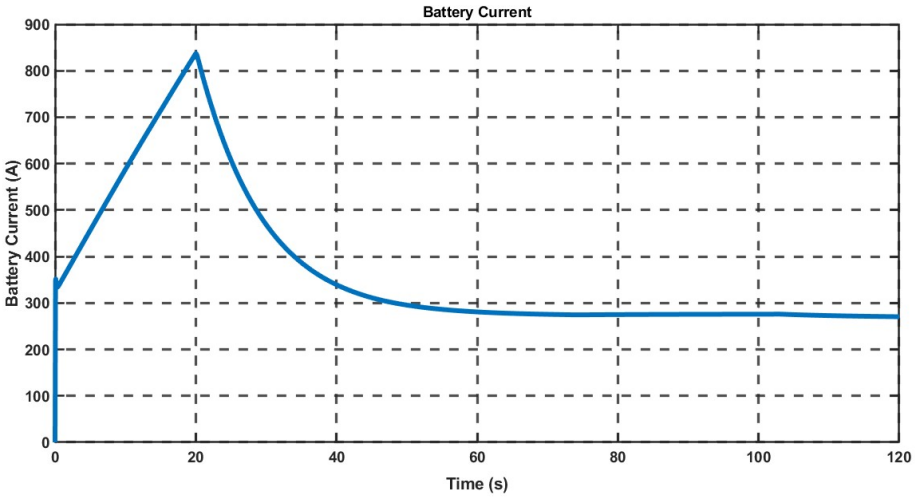


Figure II.10: Battery Current.

The SOC curve demonstrates the battery's charge level throughout the cycle, helping to assess energy consumption and regeneration performance.

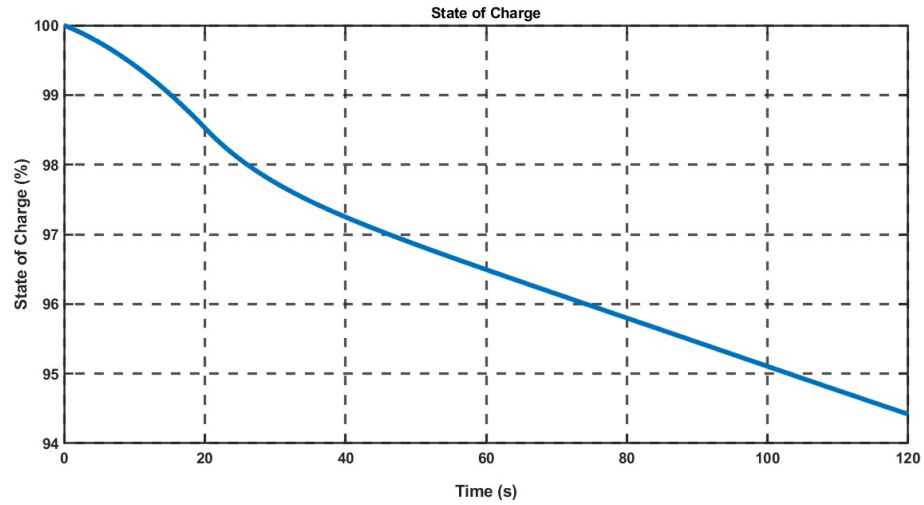


Figure II.11: State of charge.

Battery power losses are visualized next to analyze the efficiency of power delivery and internal losses.

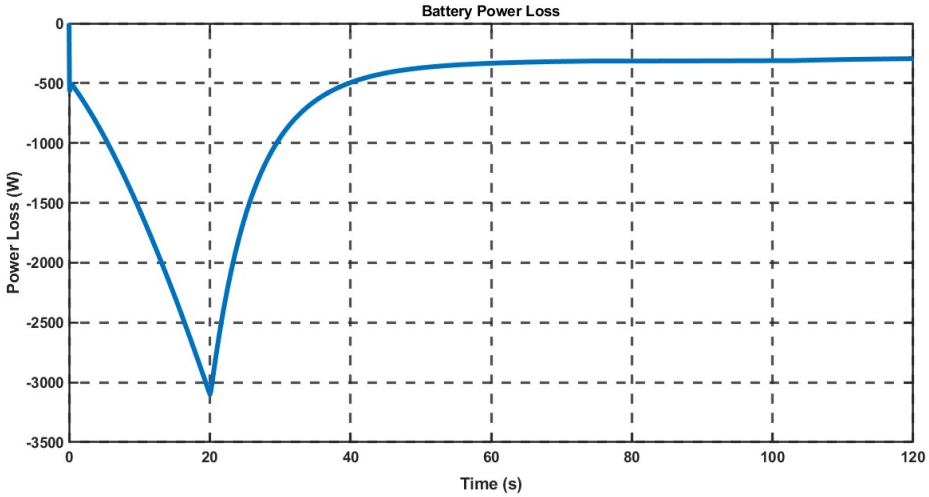


Figure II.12: Battery Power Loss.

- Battery Current peaks (800 A) initially, reflecting high acceleration demand.
- SOC declines slightly from 100% to 94%, indicating moderate energy use.
- Power Loss in Battery shows highest withdrawal at 20 seconds, decreasing afterward.

II.5.4.4 Mechanical and Electrical Power

The following figure shows the mechanical power output of the electric motor, representing the torque and speed contribution to vehicle propulsion.

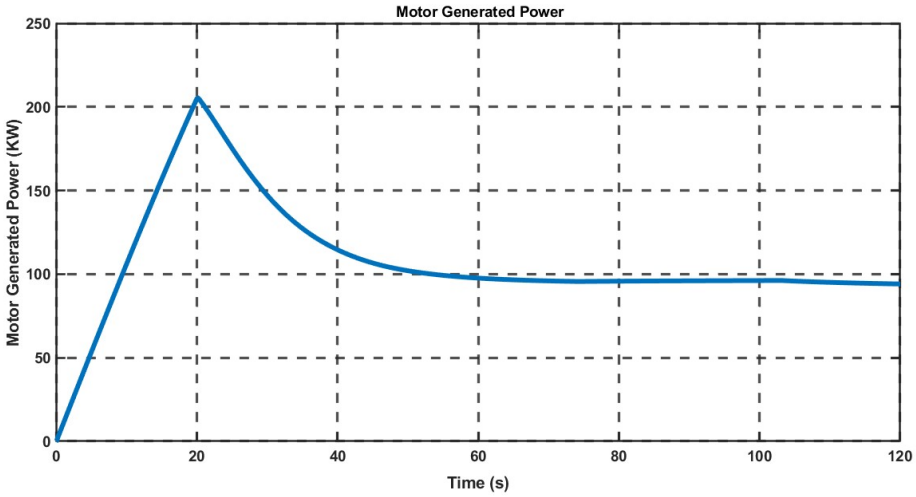


Figure II.13: Mechanical Power Generated By Motor .

The electrical power delivered to the motor is plotted below to examine the energy conversion process and electrical demand.

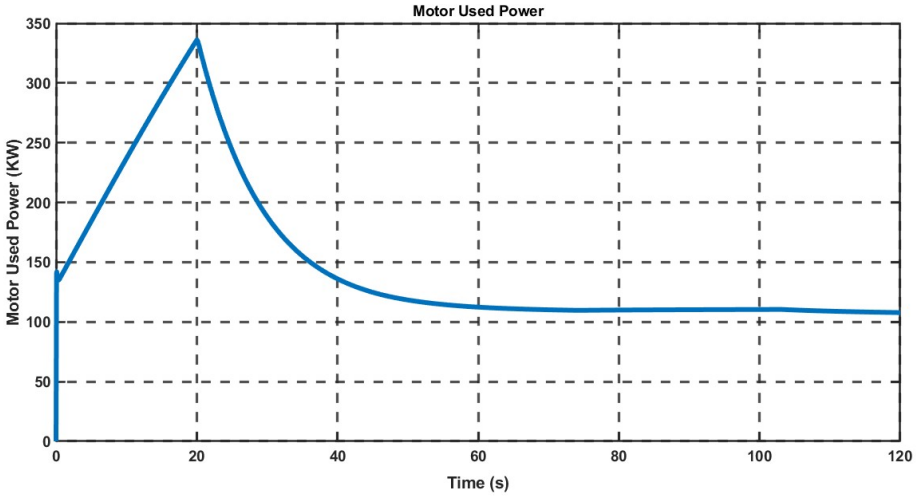


Figure II.14: Electrical Power Given To Motor.

The motor efficiency is depicted to evaluate how effectively electrical energy is converted into mechanical output under varying conditions.

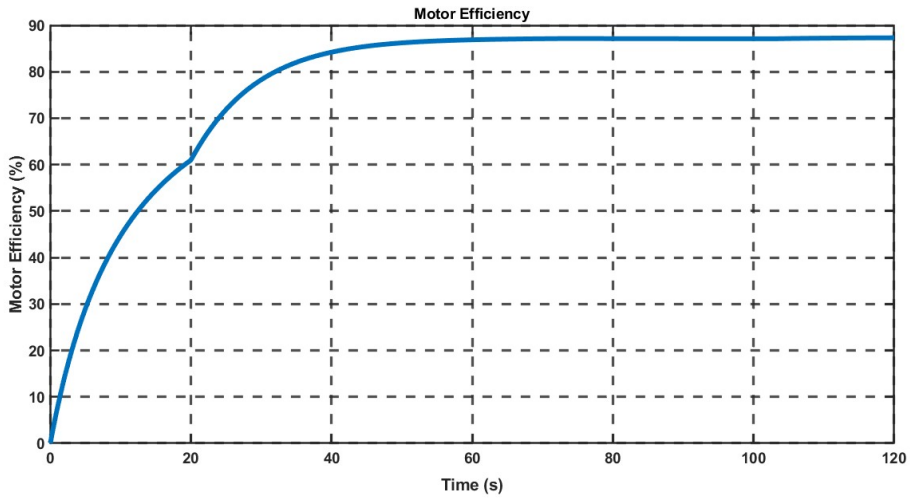


Figure II.15: Efficiency of the Motor.

- Mechanical Power reaches a peak 200 kW at around 20 seconds, rapidly decreasing afterward and stabilizing.
- Electrical Power peaks 350 kW at about 20 seconds, then stabilizes at lower values.
- Efficiency improves sharply initially, stabilizing around 87%.

II.5.4.5 Battery Sizing

With battery weight directly correlated with the number of parallel cells Np, this part evaluates the effects of Np on the performance of our BEV model.

The velocity profiles are shown to confirm that all battery sizing configurations maintain consistent speed tracking performance during the drive cycle.

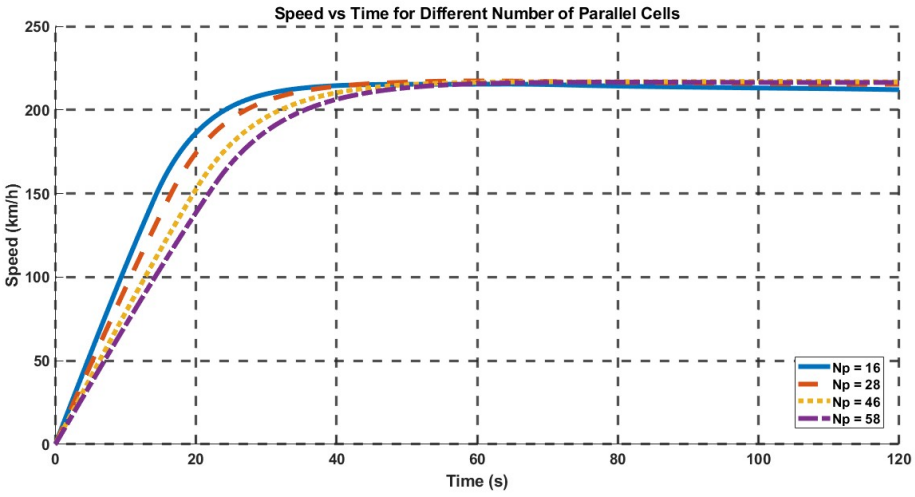


Figure II.16: Velocity For Different Np

The figure below presents the power loss in the battery for different sizing scenarios, allowing evaluation of how battery capacity impacts energy efficiency and internal losses.

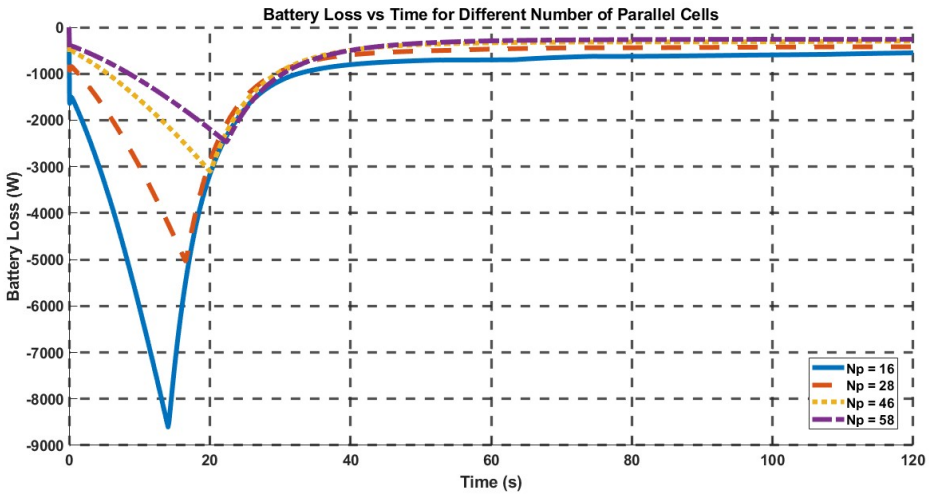


Figure II.17: Battery Power Loss For Different Np

By reducing Np, one can achieve better initial acceleration for the lighter weight, but this comes at the cost of increased power loss. On the flip side, increasing Np can lead to improved efficiency but decrease acceleration, though it does add additional weight. It is crucial to find the right Np to maintain a balance between acceleration and efficiency.

The simulation illustrates an absolute need for strong power and high torque during the initial phases of acceleration, followed by effective, steady operating at cruising speeds. Moderate usage is reflected in the battery management, which keeps efficiency and sufficient SOC throughout the simulation. Performance is greatly impacted by battery size; higher parallel cell counts lower peak power loss, provide smoother power delivery, and improve battery longevity and stability.

II.6 Conclusion

This chapter designed and simulated an electrical vehicle system, studying how several parameters, such as motor dynamics, speed profiles, and the number of parallel cells (Np), affect performance. Key consequences between acceleration, efficiency, and power loss are shown by the results, illustrating the difficulties in system design optimization. Building on these discoveries, the following chapter will discuss how to improve efficiency and control in the energy management of parallel configurations of hybrid electric vehicles (HEVs) by utilizing Model Predictive Control (MPC).

Chapter III

Energy Management Using Model Predictive Control in Parallel Hybrid Electric Vehicles

III.1 Introduction

Our modeling and simulation of a Battery Electric Vehicle (BEV) demonstrated the high efficiency that can be attained only by electric motors, but it also exposed the vehicle's range and energy storage capacity constraints. Hybrid electric vehicles (HEVs) integrate an electric motor (EM) and an internal combustion engine (ICE) into a single powertrain to solve these problems. Since ICE and EM are mechanically attached to the wheels in a parallel HEV system, they can deliver torque either separately or simultaneously, depending on driving conditions.

However, the real benefit of a parallel HEV depends on how well the energy transfers between the ICE and EM are managed. To determine the optimal way to divide the necessary driving torque between the two sources at each moment to maximize efficiency, minimize fuel consumption, and maintain battery charge, an optimized Energy Management Strategy (EMS) is necessary.

In this context, Model Predictive Control (MPC) provides an advanced method to EMS setup as it can predict future driving conditions and optimize decisions through a prediction horizon. This chapter focuses on employing an MPC-based EMS for modeling, control formulation, and simulation of a parallel HEV.

III.2 Parallel HEV Powertrain Architecture

A parallel hybrid electric vehicle (HEV) architecture allows both an electric motor (EM) and an internal combustion engine (ICE) to contribute drive torque through a shared gearbox by mechanically pairing them to the transmission input shaft. Unlike series hybrids, which use an ICE just to run a generator, the parallel configuration eliminates additional energy conversion stages, increasing overall powertrain efficiency, especially at highway speeds. the Figure III.1 illustrates the main components:

- **ICE:**produces high power at medium-to-high loads by consuming fuel to create mechanical torque on its shaft.
- **EM:**Offers rapid torque response, high efficiency at low speeds, and functions as a generator during braking.
- **Coupler/Gearbox:**a mechanical device with a fixed ratio that distributes the net torque to the wheels by combining the ICE and EM torques.

- **Battery:**Supplies DC power to the EM via a power electronics converter and stores the energy recovered during regenerative braking.

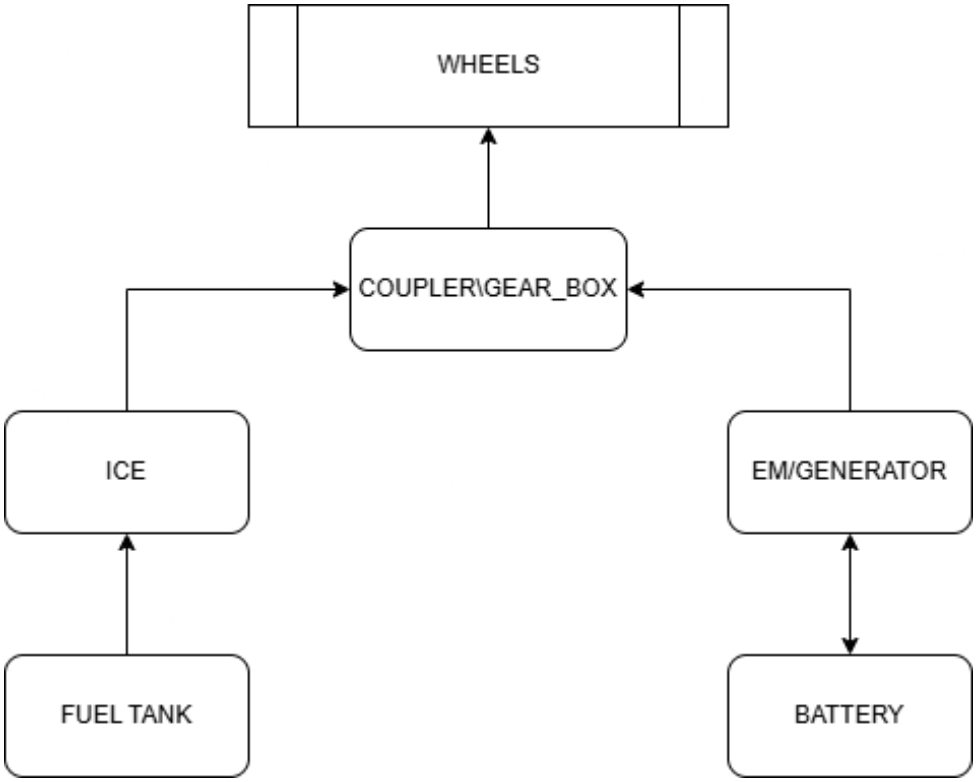


Figure III.1: HEV Parallel Configuration Architecture

This configuration supports four operating modes to optimize performance and efficiency.

- **EV Mode:**The electric motor by itself, which gets electricity from the battery, drives the car while it is moving slowly or with little load.
- **ICE Mode:**The internal combustion engine is the only source of power for the vehicle, and it operates mostly at higher, more stable speeds where it is more efficient.
- **Hybride Mode:**Together, the electric motor and engine give additional power for tasks such as lifting, accelerating, and climbing slopes.
- **Regenerative Braking Mode:**The electric motor functions as a generator to recover kinetic energy and recharge the battery when braking or decelerating.

In general, the parallel HEV configuration offers many methods of integrating the electrical motor and the engine. Managing energy flow effectively is the next crucial stage, and this is what energy management strategy are about.

III.3 Hybrid Vehicle Powertrain Model

Our MPC energy-management loop is able to operate every second by substituting a quick, map-based representation for the powertrain complexity dynamics.

III.3.1 Purpose and Overview

Our Model Predictive Control (MPC) Energy Management Strategy requires a vehicle model that can effectively forecast power and energy flows without the overhead of full dynamic simulation in order to be implemented in real-time. Detailed models that go over the time requirements of a 1 s MPC loop, such as electrical switching dynamics, drivetrain compliance, and engine and motor transients, are computationally demanding.

Rather, we use a steady-state modeling strategy. This system uses algebraic relations or pre-defined lookup maps that are evaluated at the current operating point to represent each component of the hybrid powertrain. The model moves from one equilibrium to the next, ignoring transient dynamics and capturing the gradual changes in torque, power, and state-of-charge that are most important for energy management.

These steady-state representations have been implemented using a Simulink QSS toolbox. The toolbox includes modular components for the driving cycle, gearbox torque summation, battery SOC, electric machine (EM), and internal combustion engine (ICE). Simple map lookups and algebraic computations are used by each block to deliver its output. This module operates almost instantly and gives the MPC controller the required constraint values and feedback signals at each time step.

III.3.2 Governing Equations

The torque coupler in this design divides power between the electric motor (EM) and internal combustion engine (ICE). All parts have similar angular velocities since they are mechanically connected:

$$\omega_{\mathrm{MGB}} = \omega_{\mathrm{EM}} = \omega_{\mathrm{CE}} \tag{III.1}$$

where ω_{MGB}, ω_{EM}, and ω_{CE} represent the angular velocities of the gearbox, electric motor, and combustion engine, respectively.

The mechanical power delivered through the system must also be balanced:

$$P_{\text{MGB}} = P_{\text{CE,mech}} + P_{\text{EM,mech}} \tag{III.2}$$

where P_{MGB} is the output power from the gearbox, and $P_{\text{CE,mech}}$, $P_{\text{EM,mech}}$ are the mechanical power contributions from the ICE and EM.

The battery dynamics are modeled for energy tracking using a simple algebraic equation between battery charge and power flow:

$$\dot{Q}_{\text{BT}}(k) = \frac{P_{\text{EM,mech}}(k)}{\eta_{\text{EM}} \cdot U_{\text{nominal}}} \tag{III.3}$$

where Q_{BT} is the battery charge, η_{EM} is the motor efficiency, and U_{nominal} is the nominal battery voltage.

Similarly, the fuel consumption rate is derived from the ICE mechanical power output:

$$V_{\text{CE}}(k) = \frac{P_{\text{CE,mech}}(k)}{\eta_{\text{CE}} \cdot H_u} \tag{III.4}$$

where V_{CE} is the fuel rate, η_{CE} is the engine efficiency, and H_u is the fuel's lower heating value.

III.3.3 QSS Toolbox Implementation

The QSS Toolbox Library in Simulink, which offers ready-to-use blocks for essential hybrid electric vehicle components, is used to construct the vehicle model, as seen in Figure III.2. Without requiring complex dynamic modeling, each block simulates steady-state behavior using algebraic equations or maps, making model development quick and simple.

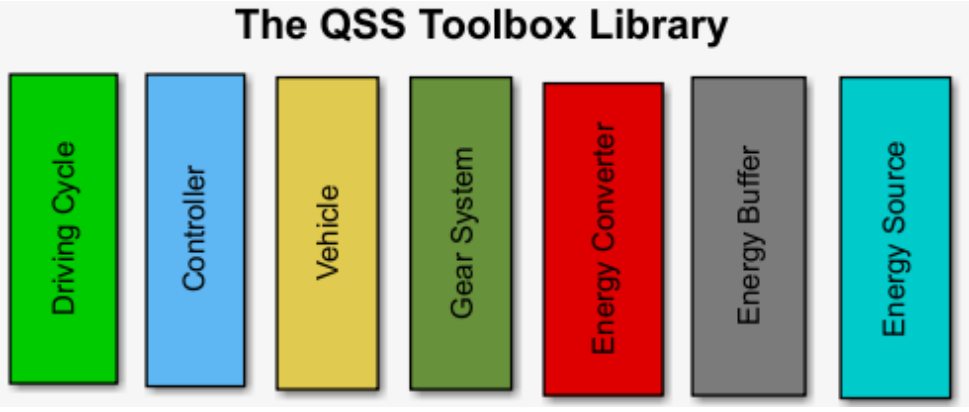


Figure III.2: QSS Toolbox Library blocks for the hybrid-vehicle.

The function of each block is the following :

- **Driving Cycle:** Supplies the reference speed or equivalent torque demand profile (e.g. NEDC, FTP-75).
- **Vehicle:** Implements resistive load torque via algebraic drag and rolling resistance formulas, enforcing the load in (Eq. III.2).
- **Gear System:** Sums ICE and EM torques and applies the fixed gear ratio, thus enforcing the equality of shaft speed (Eq. III.1) and the power balance (Eq. III.2).
- **Energy Converter:** Contains two sub-blocks with lookup tables:
  - ICE map converts (ω_{CE}, T_{CE}) to $P_{CE,mech}$ and $\dot{V}_{CE}$ through (Eq. III.4).
  - EM map converts (ω_{EM}, T_{EM}) to $P_{EM,mech}$ and enforces torque limits, feeding the SOC update in (Eq. III.3).
- **Energy Buffer:** Implements the battery SOC update (Eq. (III.3)) with a gain and integrator, tracking Q_{BT} without additional dynamic states.
- **Energy Source:** Converts engine mechanical power into fuel flow via Eq. (III.4), providing instantaneous $\dot{V}_{CE}$ for economy calculations.

The QSS Toolbox components mentioned above use steady-state algebraic relations to implement the hybrid powertrain equations. At each 1 second time step, the battery SOC and fuel flow are updated by the engine, motor, gearbox, and battery, all of which contribute to a computationally efficient plant model. Through the use of static equations or precalibrated maps instead of differential dynamics, this architecture ensures real-time execution while offering the accuracy required for predictive control. In the next part, the MPC-based Energy Management Strategy is built using this vehicle model as the prediction environment.

III.4 Energy Management Strategy

Both the electric motor (EM) and the internal combustion engine (ICE) in a parallel hybrid electric vehicle (HEV) are able to provide torque to the drivetrain. However, fuel consumption, battery life, and overall performance are greatly impacted by the timing and manner of each source's contribution. For this interaction to be well managed, an Energy Management Strategy

(EMS) is necessary [29] [30]. An EMS's primary objectives are to reduce fuel consumption, keep the battery's State of Charge (SOC) within safe bounds, and insure responsive and efficient vehicle operation.

III.4.1 Selection of MPC for Energy Management

Model Predictive Control (MPC) [12], one of the several available control techniques, has a number of benefits to manage the energy consumption of HEVs. Based on upcoming driving demands and system limits, it enables predictive decision making. MPC has the ability to apply limits, such as maximum torque or efficiency targets, while simultaneously taking into account a number of variables, including torque needs, battery state of charge, and engine operating points. MPC predicts the future behavior of the vehicle and finds the ideal torque split between the ICE and the EM by solving an optimization problem at each time step.

III.4.2 Control Flow and System Overview

Figure III.3 illustrates the structure of the MPC-based energy management strategy proposed in this work.

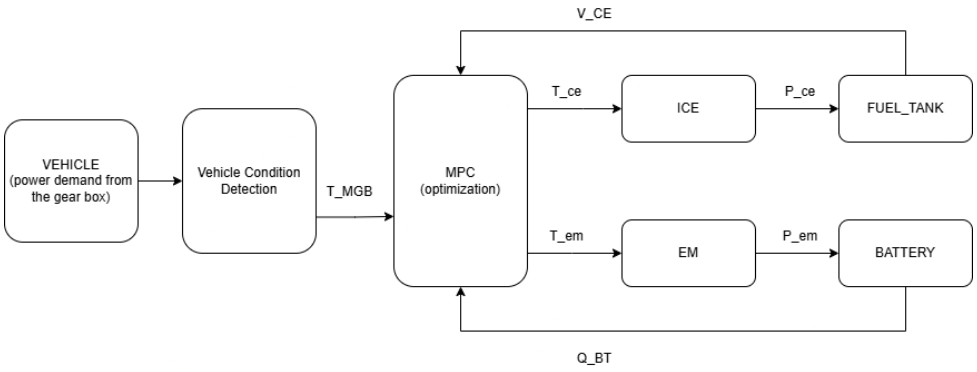


Figure III.3: Structure of the MPC Energy Management Strategy

The torque requirement of the vehicle, which is established by the present driving cycle and delivered through the manual gearbox T_{MGB}, starts the control flow. This demand is processed by a Vehicle Condition Detection block, which also gives the MPC controller the pertinent operating conditions. The MPC determines the ideal torque contributions from the ICE T_{ce} and EM T_{em} using these inputs, as well as feedback on the battery charge Q_{BT} and engine output V_{CE}.

These torque commands are converted into power P_{ce} and P_{em} by the ICE and EM respectively. This loop keeps going in real time, guaranteeing effective functioning while meeting performance requirements.

III.4.3 MPC Strategy Logic and Workflow

The Model Predictive Control (MPC) strategy operates in a receding horizon fashion. At each time step, it measures the current state of charge (SOC) and power demand, then predicts the SOC evolution over a fixed horizon using a discrete vehicle model.

A cost function is evaluated based on fuel consumption and SOC tracking error, subject to power and SOC constraints. The controller solves an optimization problem to determine the optimal power split between the electric motor (EM) and internal combustion engine (ICE). Only the first control input is applied, and the process repeats at the next time step.

Figure III.4 shows the control flow structure of the MPC-based energy management system.

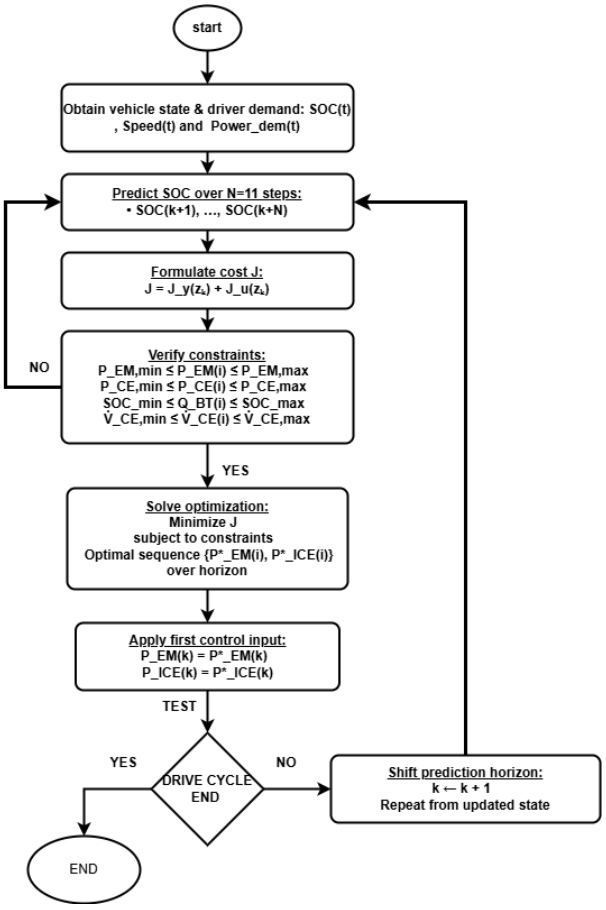


Figure III.4: Flowchart illustrating the Model Predictive Control (MPC) process for energy management in the parallel HEV.

III.4.4 MPC Formulation

The Model Predictive Control (MPC) approach solves a finite-horizon optimization problem to find the best distribution of energy between the electric motor (EM) and internal combustion engine (ICE) at each time step. In this part, the prediction model is formulated, the cost function is defined, and the set of operational and physical constraints used during optimization is presented.

III.4.4.1 State-Space Prediction Model

A linear time-invariant discrete-time state-space model is used within the MPC to predict future battery charge and fuel rate. The model has the form

$$\begin{cases} x(k+1) = A\,x(k) + B\,u(k), \\ \quad y(k) = C\,x(k) + D\,u(k). \end{cases} \tag{III.5}$$

where

$$x(k) = \begin{bmatrix} Q_{BT}(k) \\ V_{CE}(k) \end{bmatrix}, \quad u(k) = \begin{bmatrix} P_{EM,mech}(k) \\ P_{CE,mech}(k) \\ P_{MGB}(k) \end{bmatrix}, \quad y(k) = \begin{bmatrix} Q_{BT}(k) \\ V_{CE}(k) \end{bmatrix}.$$

Based on the quasi-static plant relations , the system matrices are

$$A = \begin{bmatrix} 1 & 0 \\ 0 & 1 \end{bmatrix}, \quad B = \begin{bmatrix} -\dfrac{T_s}{\eta_{EM}\,U_{nominal}} & 0 & 0 \\ 0 & \dfrac{T_s}{\eta_{CE}\,H_u} & 0 \end{bmatrix},$$

$$C = \begin{bmatrix} 1 & 0 \\ 0 & 1 \end{bmatrix}, \quad D = \begin{bmatrix} 0 & 0 & 0 \\ 0 & 0 & 0 \end{bmatrix}.$$

Here:

- The first column of B maps motor mechanical power $P_{EM,mech}$ into the SOC update.
- The second column of B maps engine mechanical power $P_{CE,mech}$ into fuel-flow rate.
- The third column is zero since the measured disturbance P_{MGB} enters via the equality constraint $P_{CE} + P_{EM} = P_{MGB}$ rather than the state update.

The sampling time is $T_s = 1$, s, with efficiencies $\eta_{EM} = 0.85$, $\eta_{CE} = 0.35$, nominal voltage $U_{nominal} = 47$, V, and is the fuel heating value

III.4.4.2 Cost Function

.

The MPC block in Simulink minimizes a standard quadratic cost composed of four terms

$$J(z_k) \;=\; J_y(z_k) \;+\; J_u(z_k) \;+\; J_{\Delta u}(z_k) \;+\; J_\varepsilon(z_k) \tag{III.6}$$

Here the decision vector

$$z_k^T = \left[u(k\,|\,k)^T,\; u(k+1\,|\,k)^T,\; \ldots,\; u(k+p-1\,|\,k)^T,\; \varepsilon_k\right]$$

collects the future control moves and slack variable. The four cost components are:

Output-tracking term

$$J_y(z_k) = \sum_{i=1}^{p} \sum_{j=1}^{n_y} w_{i,j}^{y} s_j^{y} \left[r_j(k+i\,|\,k) - y_j(k+i\,|\,k)\right]^2 \tag{III.7}$$

where

- $r_j(k+i\,|\,k)$ is the reference for output j (we choose $Q_{BT,ref} = 18000$ for charge sustainment and $\dot{V}_{CE,ref} = 0.01$ to minimize fuel).
- $y_j(k+i\,|\,k)$ is the predicted output.
- s_j^y is the scale factor for output j.
- $w_{i,j}^y$ is the tuning weight at prediction step i.
- n_y is the number of outputs and p the prediction horizon.

Input-tracking term

$$J_u(z_k) = \sum_{i=0}^{p-1} \sum_{j=1}^{n_u} w_{i,j}^{u} s_j^{u} \left[u_j(k+i\,|\,k) - u_{j,\text{target}}(k+i\,|\,k)\right]^2 \tag{III.8}$$

where

- $u_{j,\text{target}}(k+i\,|\,k) = 0$, since no explicit reference is imposed on the engine or motor power.
- s_j^u is the scale factor for input j.
- $w_{i,j}^u$ is the tuning weight for input j at step i.
- n_u is the number of manipulated inputs.

Move-suppression term

$$J_{\Delta u}(z_k) = \sum_{i=1}^{p-1} \sum_{j=1}^{n_u} w_{i,j}^{\Delta u} \left[u_j(k+i\,|\,k) - u_j(k+i-1\,|\,k)\right]^2$$

Here all $w_{i,j}^{\Delta u} = 0$, so sudden torque-split changes are not penalized.

Constraint-violation term

$$J_\varepsilon(z_k) = \sum_{\ell=1}^{n_c} w_\ell^\varepsilon \, \varepsilon_\ell(k)^2$$

Here all $w_\ell^\varepsilon = 0$, enforcing hard constraints (no slack allowed).

Tuning choices

- Charge sustainment: $Q_{BT,ref} = 18000$ (50%SOC).
- Fuel minimization: $\dot{V}_{CE,ref} = 0.01$.
- No input reference: $u_{j,\text{target}} = 0$.
- No move suppression: $w_{i,j}^{\Delta u} = 0$.
- No soft constraints: $w_\ell^\varepsilon = 0$.

With these settings, the MPC focuses exclusively on maintaining battery charge and minimizing fuel consumption, without penalizing necessary torque adjustments or permitting constraint breaches.

III.4.4.3 Constraints

The MPC must enforce hard bounds on both the manipulated variables and the output variables of the Parallel HEV plant.

$$\begin{aligned} P_{EM}^{\min} &\le P_{EM}(i) \le P_{EM}^{\max}, \\ P_{CE}^{\min} &\le P_{CE}(i) \le P_{CE}^{\max}, \\ SOC_{\min} &\le Q_{BT}(i) \le SOC_{\max}, \\ V_{CE,\min} &\le V_{CE}(i) \le V_{CE,\max}. \end{aligned} \tag{III.9}$$

The MATLAB MPC Toolbox implements the same bounds in a unified "mixed-constraint" form:

$$E\,u(k+j) + F\,y(k+j) + S\,v(k+j) \le G, \tag{III.10}$$

where

$$u = [P_{EM}, P_{CE}], \quad y = [Q_{BT}, V_{CE}], \quad v = P_{MGB},$$

and E, F, S, G are chosen so that each row of (III.10) reproduces an inequality from (III.9) when the scale factors are unity and the slack variables are zero. Thus, MPC optimization strictly enforces all physical limits of the powertrain as hard constraints.

The MPC optimization issue is now fully stated with the state-space model, cost function, and constraints in place. The controller can calculate torque set-points that follow all physical restrictions while balancing fuel consumption and SOC regulation.

III.4.5 Mode Decision Logic

The control strategy employed in the parallel HEV does not depend on fixed rules to select operating modes. Rather, the Model Predictive Control (MPC) algorithm consistently calculates optimal torque values for both the internal combustion engine (ICE) and the electric motor (EM) according to the current conditions and constraints of the vehicle. These torque values inherently dictate the vehicle's operating mode at every time interval.

- **OFF State:** Occurs when both $T_{ce} = 0$ and $T_{em} = 0$, typically during standstill or coasting. No propulsion or regeneration occurs.
- **Load Point Shifting (LPS):** Occurs when $T_{ce} > 0$, with $T_{em} \ge 0$. The ICE supplies the main torque demand; the EM may assist or remain inactive depending on efficiency.
- **Electric Driving (ED):** Occurs when $T_{ce} \approx 0$ and $T_{em} > 0$. The vehicle is powered entirely by an electric motor.

- **Regenerative Braking (REG):** Happens when $T_{em} < 0$ and $T_{ce} = 0$. The EM functions as a generator, recovering braking energy to recharge the battery.

As a result, the MPC adjusts torque outputs in response to driving demands, maintaining energy efficiency and smooth performance.

III.5 Simulation Setup

The main model parameters, controller configurations, starting circumstances, and driving cycles used in the Simulink-based hybrid vehicle simulation are described in this section.

III.5.1 Model Initial Conditions and Parameters

Realistic parameters that are compatible with a parallel hybrid electric car are used in the simulation model. The nominal capacity of the battery is 10 Ah (36 000 As). The average steady-state efficiencies of the internal combustion engine (ICE) and electric motor are $\eta_{EM} = 0.85$ and $\eta_{CE} = 0.35$, respectively. Lower heating value of the fuel is $H_u = 43$MJ/kg.

The battery SoC is set to 50% (18000 As) at the initial start of the simulation, and the fuel flow rate is set to 0.01 kg/s.

III.5.2 MPC Settings

The MPC has used a prediction horizon of $N_p = 11$ steps and a control horizon of $N_u = 2$ steps. In accordance with the simulation time step, the controller runs at a set sampling period of one second.

The simulation solver is set to **VariableStepDiscrete**, with an automatic maximum step size of 1s.

III.5.3 Drive Cycle

The New European Driving Cycle (NEDC), a standardized test technique to evaluate vehicle emissions and fuel consumption specified in UNECE Regulation No. 101. [31], was used to run the simulation.

III.5.4 Simulink Model Overview

Figure III.5 shows the Simulink layout of a parallel HEV system. It includes a driving cycle input, vehicle dynamics, gearbox, control unit, combustion engine, electric motor, battery, fuel tank, and equivalent fuel consumption blocks.

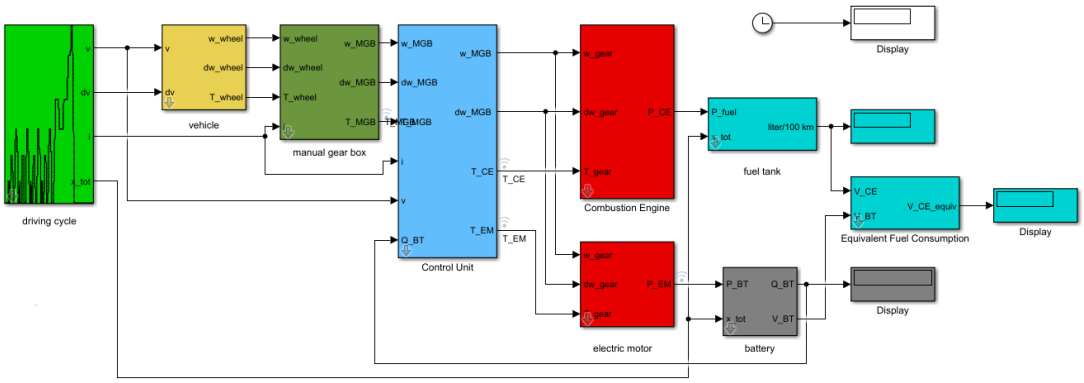


Figure III.5: Simulink model of a Parallel HEV.

III.5.5 Simulink Model Subsystem Block

Key subsystems are presented individually to clarify their roles within the overall model.

III.5.5.1 Vehicle Subsystem

The vehicle subsystem, illustrated below, combines the drive cycle input, the longitudinal vehicle dynamics, and the gearbox model. This integrated structure provides the necessary environment to evaluate vehicle response under various driving conditions.

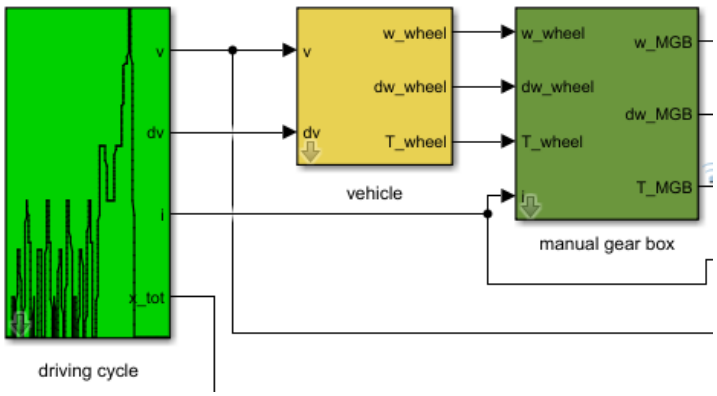


Figure III.6: Drive cycle, vehicle model, and gearbox.

This subsystem illustrates the vehicle's physical reaction to the driver's commands. The drive cycle establishes a reference speed, which the vehicle dynamics module utilizes to calculate wheel torque and speed. These values are subsequently transmitted through the manual transmission, transforming them into shaft speed and torque signals for the control unit and powertrain.

III.5.5.2 control unit

The control unit, shown below, is responsible for managing power distribution between the internal combustion engine and the electric motor. It includes the Model Predictive Control (MPC) strategy, which optimizes energy use based on system predictions and constraints.

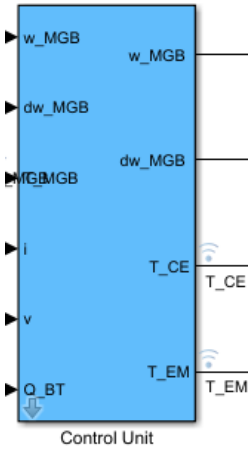


Figure III.7: MPC-based control unit.

The control unit is responsible for receiving various inputs such as gearbox speed, torque, battery state of charge (SOC), and the refernce speed. Processes these inputs using a model predictive control algorithm to identify optimal torque commands for the internal combustion engine (ICE) and the electric motor (EM), thus balancing fuel efficiency with battery health while maintaining overall performance.

III.5.5.3 Power Sources: ICE and EM

The power source subsystem, depicted below, includes the internal combustion engine (ICE) and the electric motor (EM). This block is responsible for generating the total propulsion power required by the vehicle, with both sources operating either individually or in parallel, depending on the control strategy.

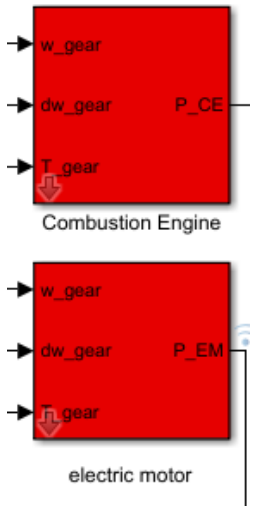


Figure III.8: Internal combustion engine and electric motor.

This aspect of the model is designed to implement the torque commands that are received from the control unit. The Internal Combustion Engine (ICE) is responsible for generating mechanical power based on inputs for torque and speed, which involves fuel consumption in the process. The electric motor (EM) improves the performance of the drivetrain by supplying electric power, which is either extracted from the battery or returned to it, depending on the demand and the state of charge (SOC).

III.5.5.4 Energy Storage and Fuel Tank

The energy storage subsystem, shown below, consists of the battery and fuel tank blocks. The battery stores electrical energy used by the electric motor, while the fuel tank supplies the internal combustion engine, ensuring continuous power availability throughout the drive cycle.

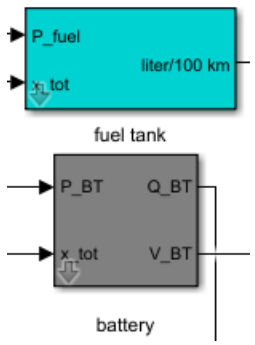


Figure III.9: Battery and fuel tank.

III.6 Simulation Results and Discussion

In this section, the principal outcomes of the MPC-based energy management strategy are presented and analyzed. We first discuss the general behavior over the full NEDC cycle, before delving into a focused examination of critical driving segments.

III.6.1 General Results

The figure below shows the vehicle's velocity response under the MPC strategy, demonstrating its ability to follow the reference speed profile accurately.

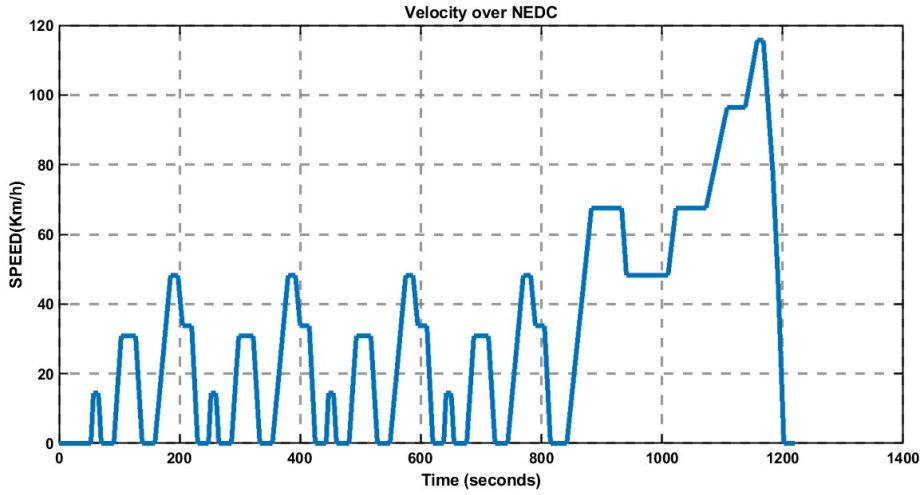


Figure III.10: Vehicle Speed Profile Over NEDC Driving Cycle (0–1220s).

Driving Cycle Dynamics: The vehicle's speed profile during the complete NEDC (0–1220 s) shows considerable fluctuations, featuring regular acceleration and deceleration phases, as well as a distinct high-speed segment towards the end of the cycle. This emphasizes the importance of having a controller that can adjust in real time to different power demands.

The following figure illustrates the torque split between the internal combustion engine and the electric motor. It demonstrates how the MPC strategy dynamically distributes the torque demand to optimize fuel economy and energy efficiency while satisfying the vehicle's performance requirements.

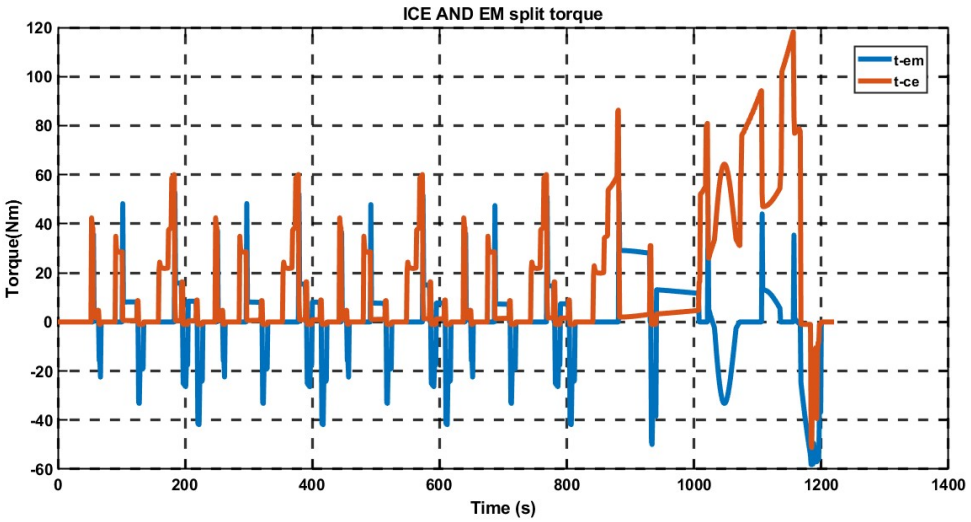


Figure III.11: Engine and Motor Torque Distribution Throughout Driving Cycle.

Torque Distribution Behavior:

- ICE Torque remains steadily positive throughout the cycle, supplying the baseline propulsion power.
- EM Torque alternates between positive (traction) and negative (charging) values. from 1030 s to 1065 s , the EM operates mainly in charging mode—an MPC response to low SOC.

The SOC profile is presented to evaluate how the MPC controller manages battery energy over time, ensuring it stays within operational limits.

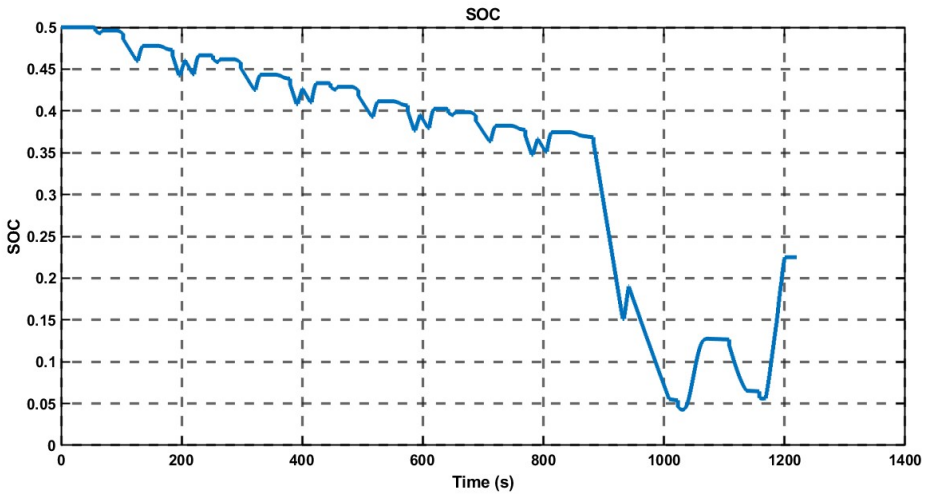


Figure III.12: Battery State of Charge.

The SOC plot shows that the MPC strategy allows the battery to discharge gradually during normal operation. Once the SOC drops below a certain limit, the controller responds by initiating charging to restore the SOC to a safer level.

The figure below presents the battery State of Charge (SOC) alongside the activation of the regenerative braking mode. This plot highlights the contribution of regenerative braking to battery recharging, as managed by the MPC strategy during deceleration phases.

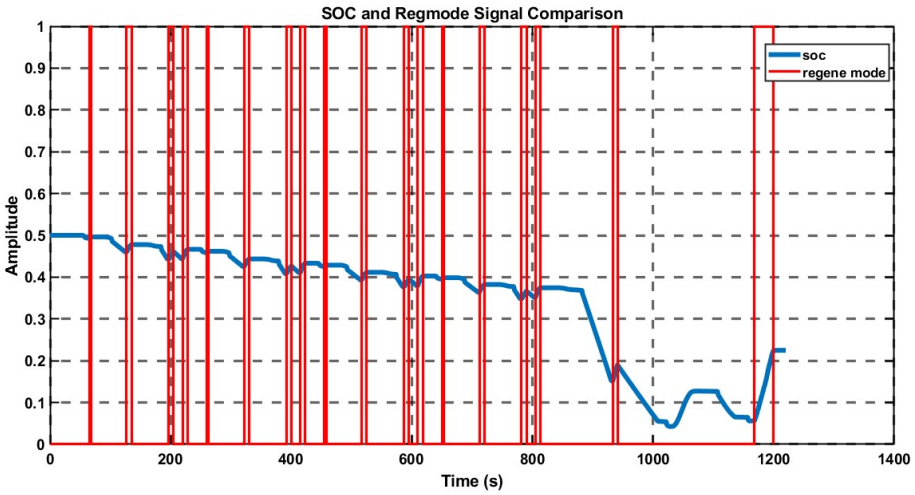


Figure III.13: Battery State of Charge with MPC-Controlled Charging Events (0–1220s).

State of Charge (SOC) Trajectory: Regenerative braking alone does not fully replenish the battery: SOC dips gradually until MPC invokes active ICE-driven charging between 1030 s and 1065 s. This confirms the MPC's capability to maintain SOC within desired limits.

The following figure illustrates the fuel consumption of the internal combustion engine during the drive cycle.

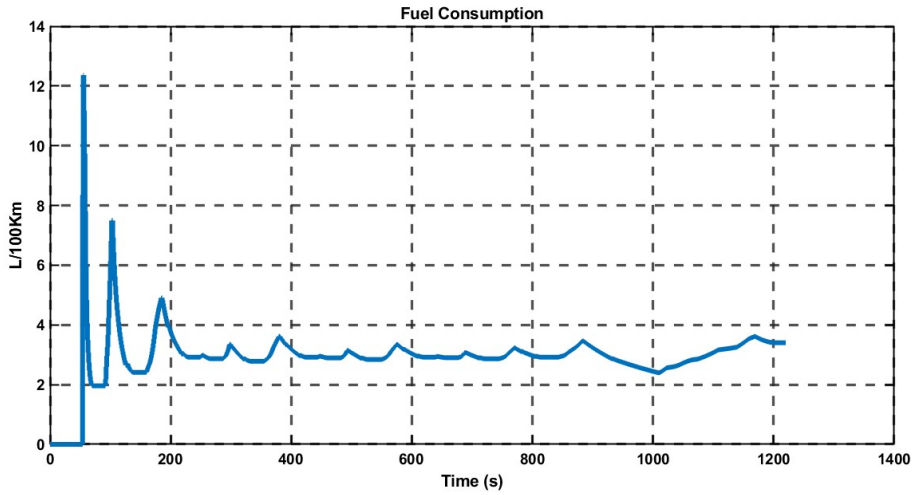


Figure III.14: Instantaneous Fuel Consumption (L/100km) Under MPC Strategy.

Instantaneous Fuel Consumption: the L/100 km curve spikes coincide with high-torque demands, especially during the late-cycle charging period. Overall consumption remains moderate given the frequent use of the EM assist, which shows how the MPC balances fuel use against torque requirements.

The following figure presents the operating modes of the hybrid electric vehicle throughout the drive cycle. It illustrates how the control strategy manages transitions between electric-only, engine-only, hybrid drive, and regenerative braking modes to ensure optimal performance and energy efficiency.

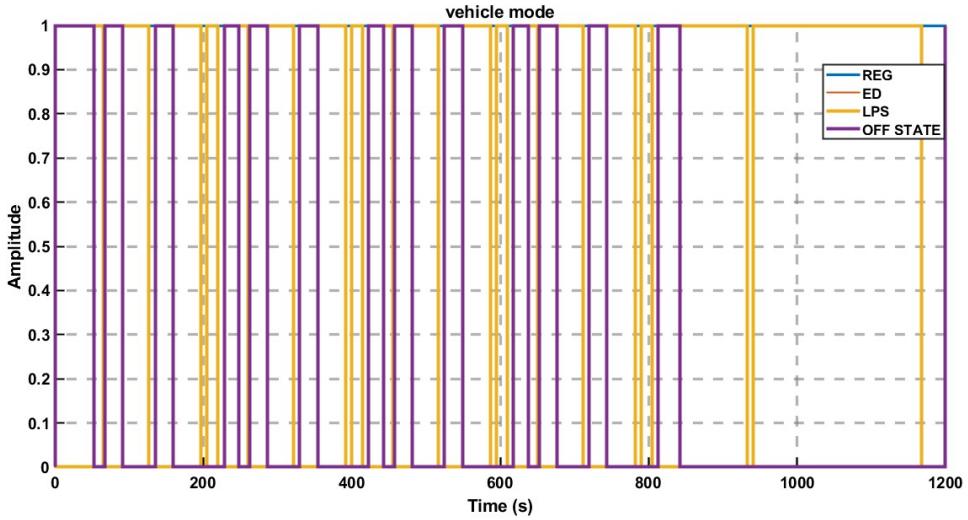


Figure III.15: Operating Modes Timeline

Operating Mode Timeline:

The MPC results show four defined modes:

- **LPS (Load-Point Shift)**: ICE operates at its optimal efficiency point, either alone or with EM assist. Most of the cycle is spent in this mode, and many LPS segments approach pure electric drive but retain minimal ICE activity under MPC.
- **EM-only (Electric Drive)**: pure electric propulsion. Inactive throughout the NEDC cycle due to the initial SOC of 50% and the MPC cost weights, which prevent coercion into purely electric segments.
- **REG (Regenerative Braking)**: EM acts as a generator during deceleration to recharge the battery.
- **OFF**: Neither ICE nor EM delivers torque, corresponding to idle or zero-demand periods.

III.6.2 Zoomed-In Analysis (800–1 220 s)

The figure below presents a zoomed-in view of the vehicle velocity during a period where battery charging occurs in the absence of regenerative braking. The speed remains relatively stable, indicating that charging is not triggered by deceleration.

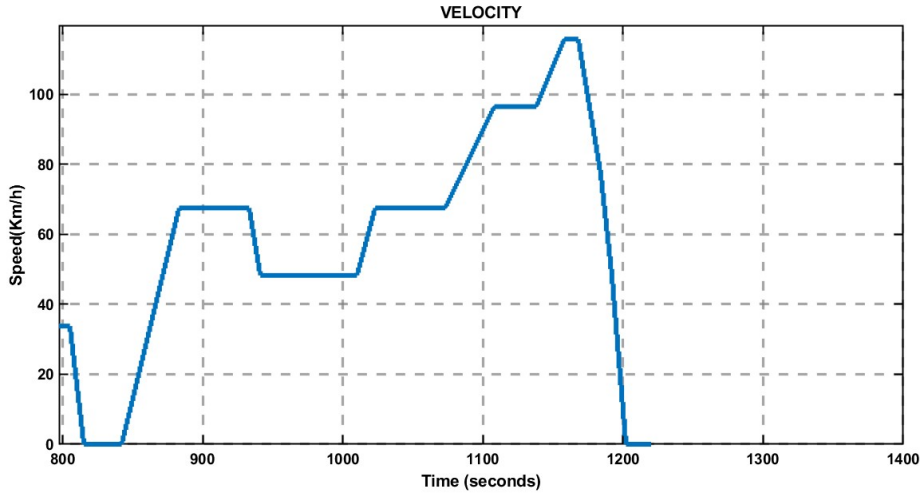


Figure III.16: Zoomed Vehicle Speed (800–1220s) Highlighting High-Speed Demand.

The corresponding torque plot, shown below, highlights how the engine or motor delivers positive torque during this phase. This confirms that the battery is charged using available mechanical power, rather than through regenerative braking.

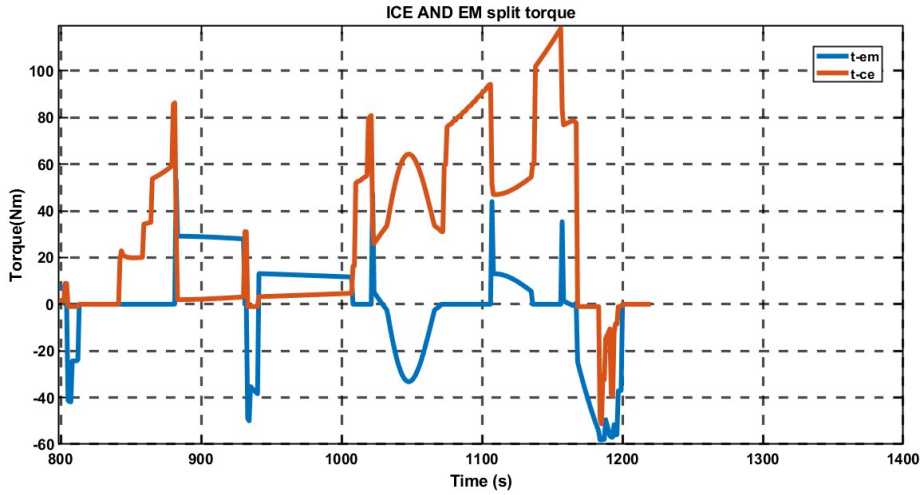


Figure III.17: Zoomed ICE and EM Torque Split (840–1220s).

Charging Phase without Regenerative Braking (1030–1065 s): In this high-speed, constant-velocity interval, MPC proactively increases ICE torque above the propulsion requirement. The

surplus mechanical power is directed to the EM, which operates as a generator, absorbing energy to recharge the battery independently of deceleration. Fig. III.17 shows a clean increase in the ICE torque at 1030 s and a matching negative EM torque (charging) profile through 1065 s, all with minimal overshoot. This behavior demonstrates MPC's ability to plan and execute charging maneuvers under steady-drive conditions.

III.7 Conclusion

In this chapter, a model predictive control (MPC)-based energy management strategy was implemented and tested for a parallel HEV over the NEDC cycle. The MPC effectively coordinated ICE and EM torque to meet driver demand while suppressing fuel consumption spikes and maintaining SOC within set limits, even scheduling ICE-driven charging during steady high-speed cruising. Although the pure EM-only mode remained inactive (initial SOC 50% and cost weights), many LPS intervals closely resembled electric driving. The mode transitions between LPS, REG, and OFF were seamless. In general, the MPC approach demonstrated clear improvements in fuel economy, SOC stability, and dynamic performance compared to conventional rule-based strategies. Chapter 4 will turn to a different approach: the design and evaluation of an Equivalent Consumption Minimization Strategy (ECMS) for a P2 HEV architecture.

Chapter IV

Energy-Management System for a P2-Parallel HEV

IV.1 Introduction

Hybrid Electric Vehicle (HEV) architectures combine an internal combustion engine and an electric machine to meet stringent emission regulations and the growing demand for fuel-efficient transportation. At the heart of HEV efficiency lies the Energy Management System (EMS), which must allocate torque in real time to minimize fuel use while preventing over-charge or depletion of the battery. In this chapter, we focus on a fixed ECMS factor of equivalence for a P2 parallel HEV: The equivalence factor s is chosen offline to ensure zero net SoC drift over a reference drive cycle, then used as the initial value in a lightweight one-step advance control law. The simulation results demonstrate that this simple strategy maintains charge balance, achieves competitive fuel economy, and drives the powertrain through its most efficient operating points.

IV.2 P2-Parallel HEV Architecture

In the P2-parallel configuration, the electric machine (EM) is mounted on the input shaft of the gearbox, between the internal combustion engine (ICE) and the transmission Figure IV.1.

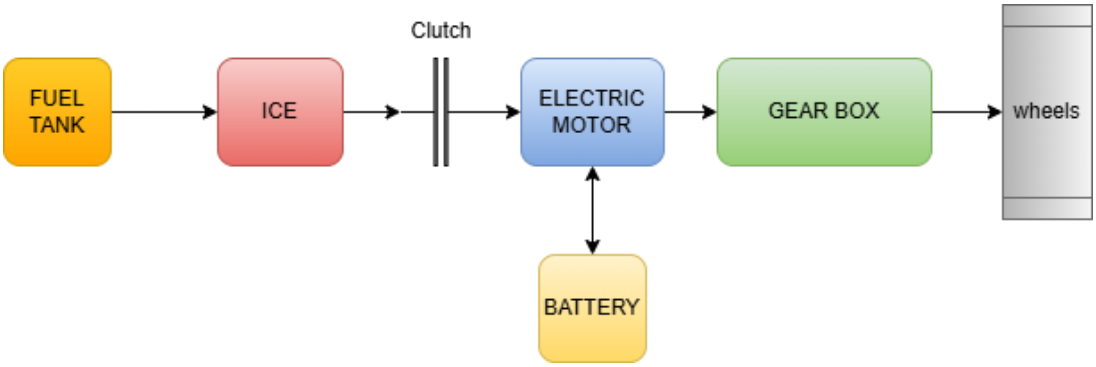


Figure IV.1: Architecture of the P2-parallel HEV .

A two-position clutch connects or disconnects the ICE crankshaft, enabling four primary operating modes:

- **Electric-Only (EV) Mode:** Clutch open, ICE off, EM drives the wheels using battery power.
- **Hybrid Mode:** Clutch closed, both ICE and EM contribute torque.
- **Engine-Only Mode:** Clutch closed, EM idle; ICE alone provides propulsion.

- **Regeneration Mode:** EM recovers kinetic energy during braking to charge the battery.

This architecture supports bidirectional power flow through the gearbox and enables smooth transitions between operating modes while leveraging existing drivetrain components.

Table IV.1: Key Simulation Parameters

Parameter	**Value**
Vehicle mass	1700 kg
Aerodynamic drag area	0.8 m^2
Rolling resistance coefficient	0.012
Wheel radius	0.22 m
Number of gears	6
Motor efficiency	0.90
Battery open-circuit voltage	350 V
Battery internal resistance	0.8 Ω
Battery charge capacity	36,000 As
State-of-charge range	20–80 %
Initial state-of-charge	60 %

IV.3 Equivalent Consumption Minimization Strategy (ECMS)

The energy management challenge in HEVs can be expressed through various performance metrics and state variables, contingent upon the specific control goals such as fuel efficiency, emissions, or battery longevity. In this study, we use the Equivalent Consumption Minimization Strategy (ECMS), a recognized instantaneous optimization method that harmonizes fuel and electric energy consumption in real-time. ECMS introduces the notion of an equivalence factor s, which converts battery energy consumption into a corresponding fuel cost. This enables the controller to minimize a consolidated cost function, irrespective of whether energy is sourced from the ICE or the EM. The instantaneous cost defined as the Hamiltonian H integrates actual fuel usage with the equivalent electrical energy expense and is minimized at every time interval to ascertain the optimal power distribution. The approach assesses both engine-on and engine-off scenarios, choosing the mode and power settings that yield the lowest total cost. Since ECMS functions at each moment without the need for a long-term driving cycle predic-

tion, it is ideally suited for real-time application and seamlessly adjusts to fluctuating driving conditions [13] [32].

To provide a clear understanding of the decision-making structure in ECMS, a simplified flowchart is presented in Figure IV.2.

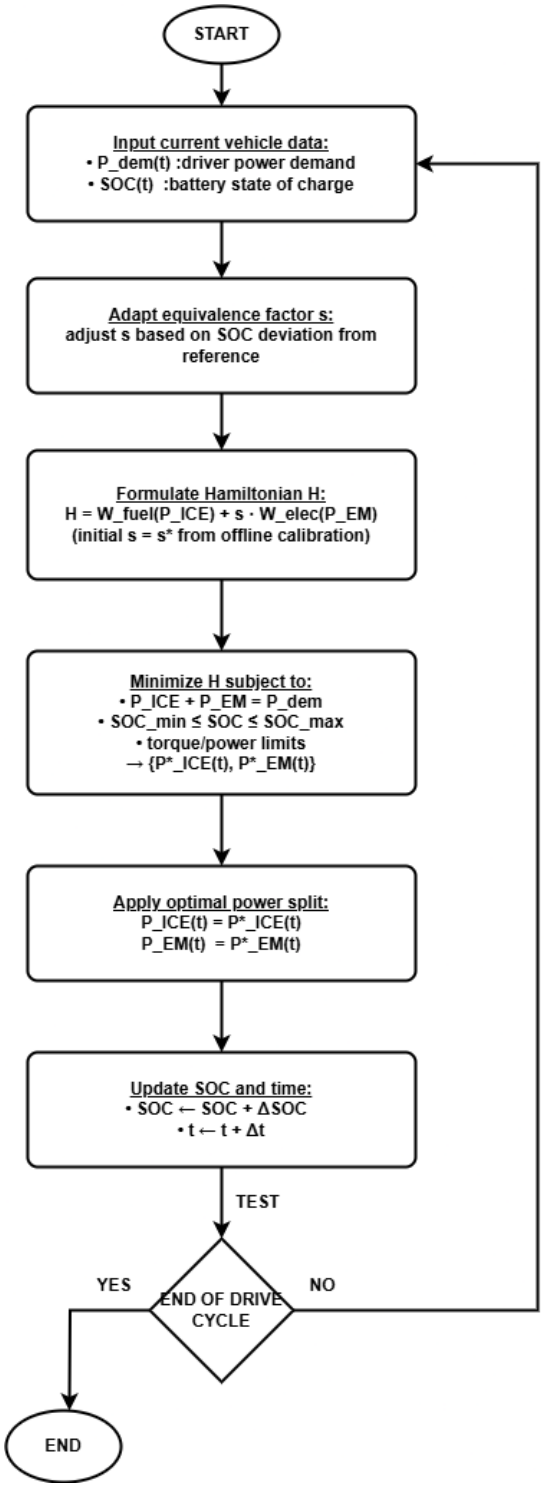


Figure IV.2: Flowchart of the Equivalent Consumption Minimization Strategy (ECMS) for real-time energy management.

IV.3.1 Instantaneous Hamiltonian

To execute the ECMS, the control objective is articulated through the Hamiltonian, which integrates both fuel consumption and electric energy usage into a unified equivalent fuel unit. This real-time formulation enables the controller to assess and reduce energy costs at each time step according to present conditions, eliminating the need for future forecasts. The subsequent expression delineates the Hamiltonian employed in the real-time optimization procedure:

$$H \;=\; L\big(u(t),w(t)\big) \;+\; \lambda\, f\big(u(t),w(t)\big), \tag{IV.1}$$

with

$$L\big(u(t),w(t)\big) = \dot{m}_f\big(w(t),u(t)\big), \qquad f\big(u(t),w(t)\big) = \frac{d\,\mathrm{SoC}}{dt} = -\frac{I_b}{Q_0}. \tag{IV.2}$$

Substituting gives

$$H = \dot{m}_f \;+\; \lambda\Big(-\frac{I_b \times V_{\mathrm{oc}}}{Q_0 \times V_{\mathrm{oc}}}\Big). \tag{IV.3}$$

Multiplying through by the fuel lower-heating-value (LHV) and using

$$P_{\mathrm{fuel}} = \dot{m}_f\,\mathrm{LHV}, \quad P_{\mathrm{bat}} = I_b V_{\mathrm{oc}},$$

we obtain unchanged Hamiltonian

$$H = P_{\mathrm{fuel}} \;-\; s P_{\mathrm{bat}}, where \quad s = -\frac{\lambda\,\mathrm{LHV}}{Q_0 V_{\mathrm{oc}}}. \tag{IV.4}$$

Finally, for a demanded torque T_{dem}, ECMS solves at each step

$$\min_{T_{\mathrm{ICE}}+T_{\mathrm{EM}}=T_{\mathrm{dem}}} \big\{\, P_{\mathrm{fuel}}(T_{\mathrm{ICE}}) \;-\; s P_{\mathrm{bat}}(T_{\mathrm{EM}})\big\}, \tag{IV.5}$$

This one-step minimization is causal and lightweight.

where

$\dot{m}_f$ fuel mass flow [g/s],

I_b battery current [A],

Q_0 battery capacity [As],

V_{oc} open-circuit voltage [V],

P_{fuel} fuel power [W],

P_{bat} battery (chemical) power,

LHV lower heating value of fuel [J/kg],

λ SoC costate (adjoint variable).

IV.3.2 Offline Determination of the Equivalence Factor

An initial coarse *tâtonnage* (trial-and-error) stage identified that the charge-sustaining equivalence factor lies near $s \approx 2.914$. We then performed a fine sweep over the interval $[2.9140, 2.9150]$ with step size 0.0001. For each candidate s_i, the WLTC drive cycle (three repeats) was simulated and the net state-of-charge change computed as

$$\Delta\text{SoC} = \text{SoC}_{\text{end}} - \text{SoC}_{\text{start}}.$$

Exactly one value yielded $\Delta\text{SoC} = 0$, indicating perfect charge-sustaining behavior. This optimal factor,

$$s^* = 2.9145$$

was adopted as the constant equivalence factor (set via `s_init`) for all subsequent ECMS simulations.

IV.4 Simulation Model Overview

Figure IV.3 presents the full closed-loop Simulink implementation of the P2-parallel HEV with fixed-s ECMS:

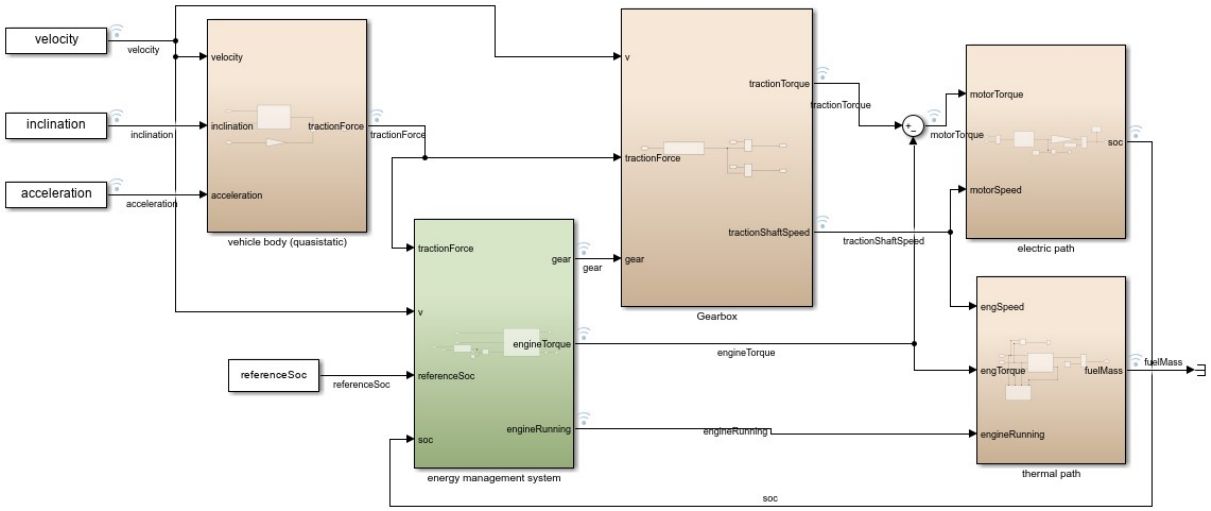


Figure IV.3: Simulink block diagram of the P2-parallel HEV model.

- **Vehicle Dynamics:** Computes traction force from driver-demanded acceleration, aerodynamic drag, rolling resistance, and incline.
- **EMS Controller:** Performs the one-step Hamiltonian minimization $H = P_{\text{fuel}} - sP_{\text{bat}}$ to split torque between ICE and EM.
- **Gearbox:** Maps traction force and vehicle speed to engine and motor shaft torques and speeds via the fixed gear ratios.
- **Electric Subsystem:** Applies motor torque, calculates electrical power exchange, and updates battery SoC.
- **Thermal Subsystem:** Applies engine torque, computes instantaneous fuel consumption based on engine operating conditions, and integrates it over time to determine total fuel mass.

This architecture captures both mechanical and electrical power flows, allowing direct evaluation of SoC trajectories, fuel consumption, and power-split dynamics under the ECMS.

IV.5 Simulation Results and Discussion

The ECMS-based energy management strategy was evaluated over a repeated WLTC drive cycle to assess its performance in a P2-parallel HEV configuration under ideal (0 drag) and realistic (0.05 drag) conditions.

IV.5.1 Drive Cycle and Power Distribution

The figure below shows the vehicle velocity profile over three successive repetitions of the WLTC drive cycle. This extended test scenario is used to assess the controller's ability to maintain accurate speed tracking over prolonged driving conditions.

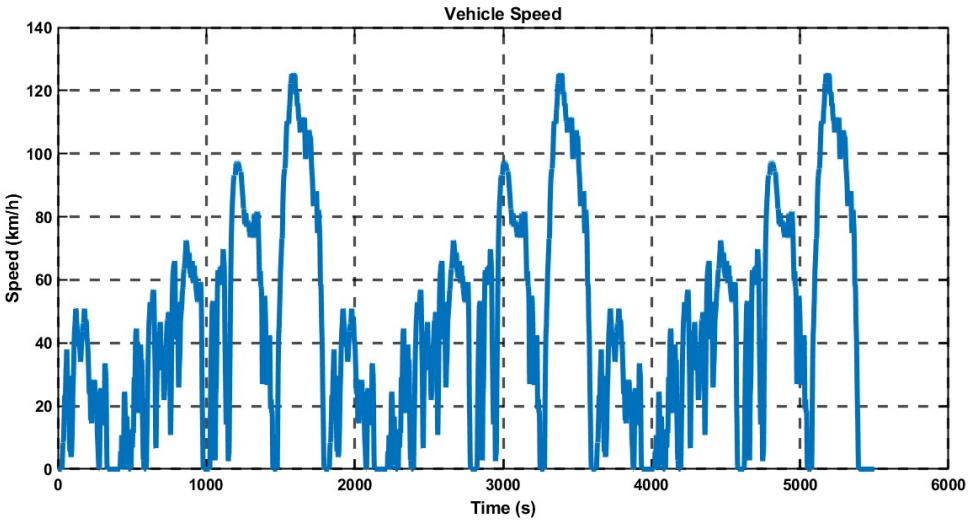


Figure IV.4: WLTC drive cycle profile repeated over three iterations.

Figure IV.4 presents the WLTC cycle repeated over three iterations to simulate extended and variable real-world driving conditions. This cycle contains urban, suburban, and high-speed segments that test the flexibility of the ECMS strategy.

The figure below depicts the torque distribution between the internal combustion engine and the electric motor during the three WLTC repetitions. It highlights how the controller optimizes power sharing over time to reduce fuel consumption while maintaining performance.

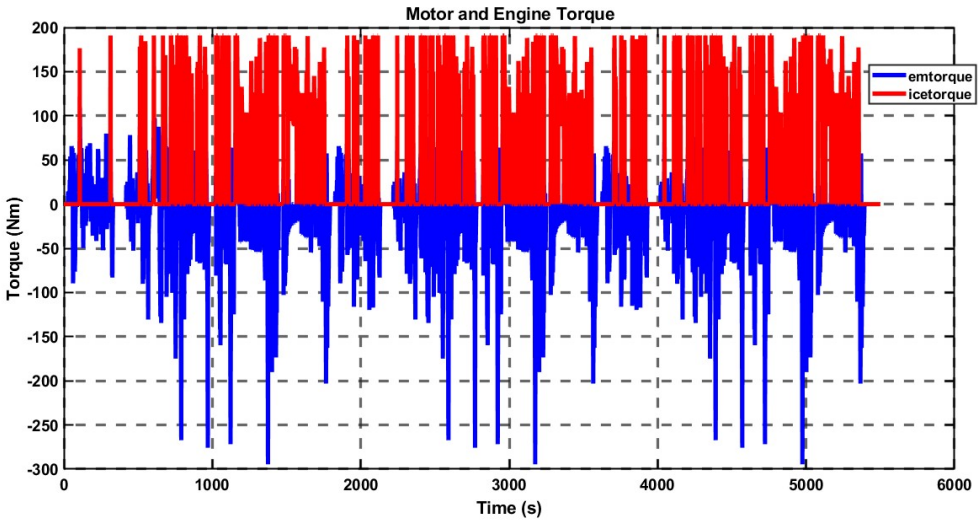


Figure IV.5: ICE and EM torque profiles over the three WLTC cycle.

As shown in Figure IV.5, the ECMS coordinates the torque between the ICE and EM based on power demand and energy cost. The ICE provides steady propulsion during high-load segments, while the EM contributes during acceleration and assists in energy recovery.

IV.5.2 Fuel Consumption and Equivalence Factor Behavior

The following figure presents the fuel consumption profile across the three repeated WLTC cycles. This result highlights the effectiveness of the control strategy in minimizing fuel usage over extended driving, while maintaining acceptable vehicle performance and battery usage.

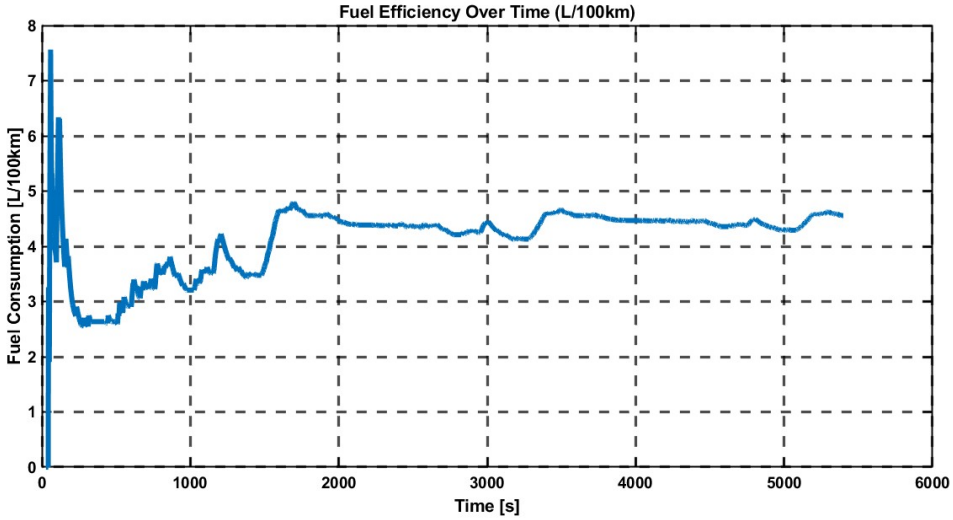


Figure IV.6: Fuel consumption over the three WLTC cycle.

Figure IV.6 shows increases in fuel consumption during acceleration and hill like segments.

However, the ECMS works to minimize overall usage by optimally managing power flow.

The evolution of the equivalence factor s is shown below. This adaptive parameter plays a key role in ECMS by adjusting the balance between fuel and electrical energy consumption in real time, ensuring optimal energy management as the driving conditions evolve.

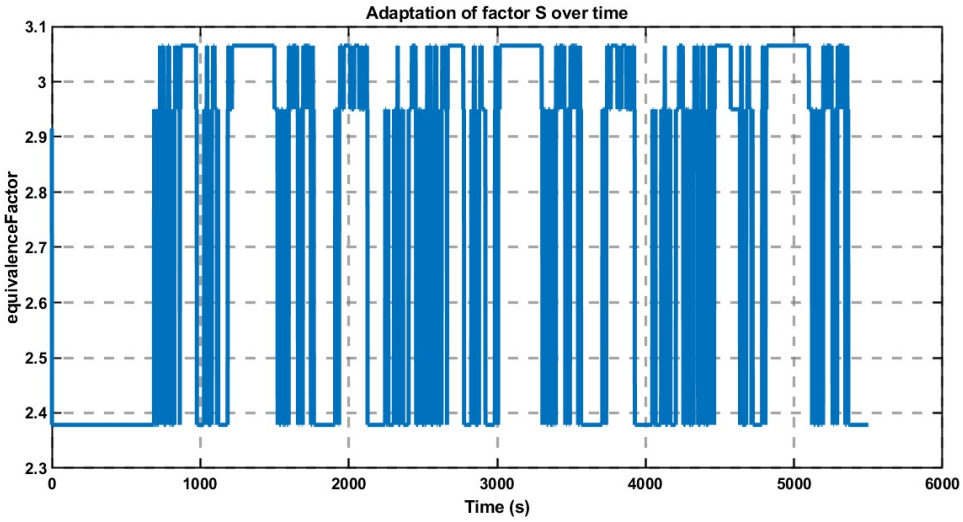


Figure IV.7: Dynamic behavior of the equivalence factor s.

Figure IV.7 displays the variation of the equivalence factor *s*, which dynamically adjusts the trade-off between fuel and electric energy. Its fluctuation reflects the ECMS's responsiveness to SOC status and power demands.

IV.5.3 Fixed vs Adaptive s Comparison No Road Load (0 Drag)

The figure below compares the battery State of Charge (SOC) evolution using fixed and adaptive equivalence factor strategies under no road load conditions. This comparison demonstrates how the adaptive s allows more flexible energy management by adjusting the electric/fuel trade-off, resulting in smoother and more balanced SOC behavior over time

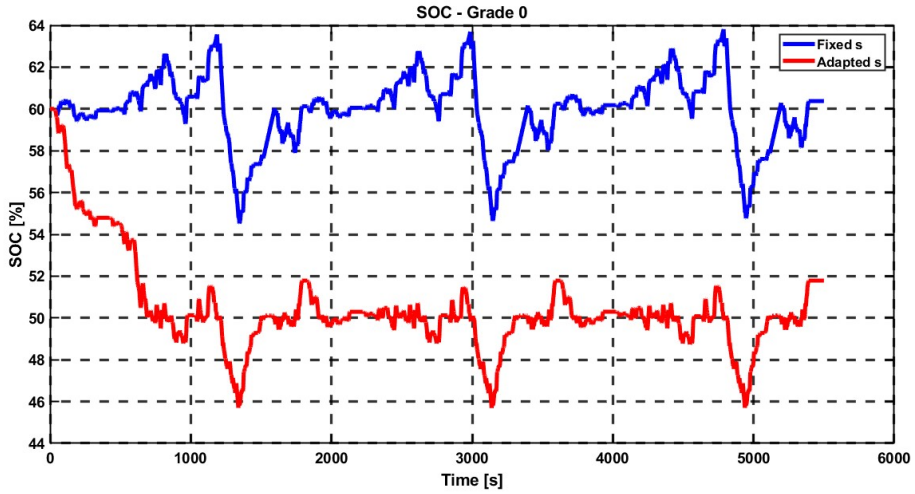


Figure IV.8: SOC trajectory for fixed and adaptive s (0 drag case).

Figure IV.8 compares the SOC profiles for fixed and adaptive *s* when no additional drag is applied. The adaptive *s* strategy maintains the SOC closer to the refernce value, showing improved energy balance.

The figure below presents the fuel consumption profiles for both fixed and adaptive equivalence factor *s* strategies under no road load conditions. The results highlight the advantage of the adaptive approach in reducing fuel usage by continuously adjusting the power split according to system state and driving conditions.

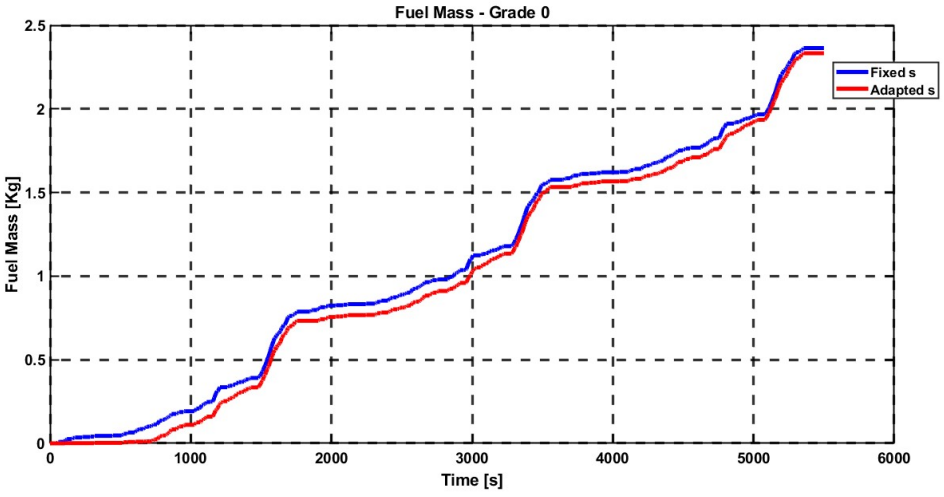


Figure IV.9: Fuel consumption: adaptive s vs fixed s (0 drag).

As seen in Figure IV.9, adaptive *s* results in lower fuel consumption compared to the fixed approach. This confirms the benefit of adjusting the equivalence factor in real-time even under ideal driving conditions.

IV.5.4 Fixed vs Adaptive s Comparison With Road Load (0.05rad Drag)

The following figure compares the SOC evolution for fixed and adaptive equivalence factor strategies under realistic road load conditions. With external resistances included, the adaptive *s* approach continues to provide more balanced SOC control, preventing over-discharge and improving battery management across the drive cycle.

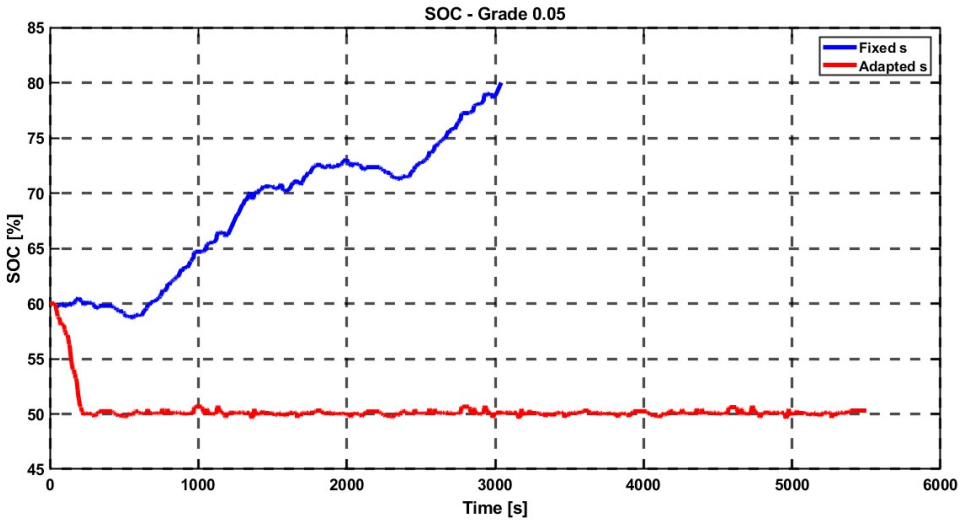


Figure IV.10: SOC trajectory for fixed and adaptive *s* (drag = 0.05).

In the presence of aerodynamic drag, Figure IV.10 shows that fixed *s* causes significant SOC deviation, whereas adaptive *s* maintains a more controlled SOC range. This highlights the strategy's robustness under increased load.

The fuel consumption results for the same scenario are shown below. Under road load conditions, the adaptive strategy demonstrates its ability to further reduce fuel usage by dynamically adjusting the power split in response to changing load demands.

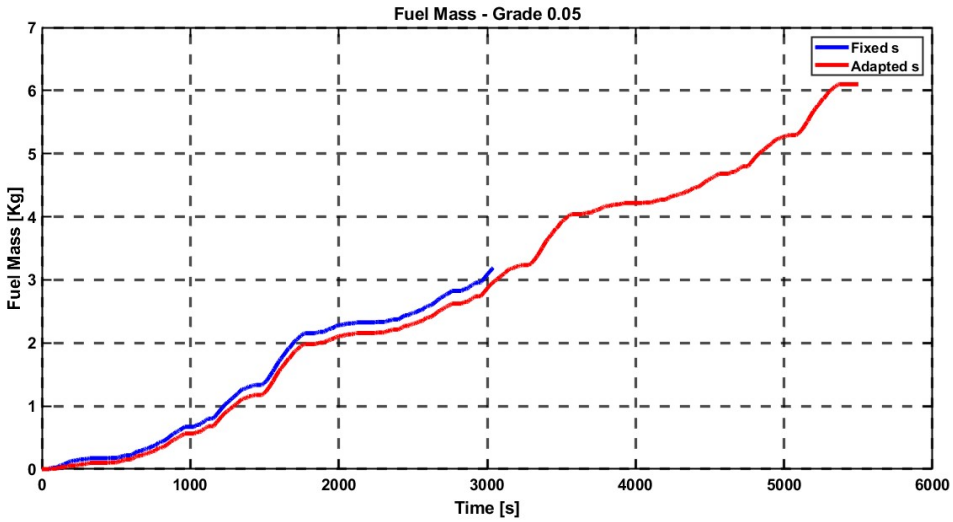


Figure IV.11: Fuel consumption: adaptive s vs fixed *s* (0.05rad Drag).

Figure IV.11 confirms that adaptive *s* continues to offer better fuel efficiency even under realistic drag conditions, proving the value of real-time adaptation.

IV.6 Conclusion

In this chapter, the Equivalent Consumption Minimization Strategy (ECMS) was applied and assessed for a P2-parallel HEV architecture. The performance of the controller was evaluated under various operating conditions through repeated WLTC cycles. The findings indicated that ECMS effectively regulates the energy distribution between the internal combustion engine and the electric motor by minimizing a fuel-equivalent cost function in real time. By incorporating an adaptive equivalence factor, the strategy responded dynamically to fluctuating load conditions and battery state, resulting in enhanced fuel economy and improved SOC maintenance compared to a fixed s approach. The advantages of adaptation became particularly apparent under increased aerodynamic drag, where the fixed-s method resulted in greater SOC drift and elevated fuel consumption. In summary, the adaptive ECMS approach demonstrated itself to be a robust and efficient solution for real-time energy management in P2 HEVs, providing a practical balance between fuel efficiency and battery utilization under diverse driving conditions.

General Conclusion

This thesis has explored the design, modeling, and control of electric and hybrid vehicles, concentrating on energy management strategies to boost efficiency and sustainability. It commenced with a broad examination of HEVs, then moved on to simulating a BEV model, applying a Model Predictive Control (MPC) framework, and finally utilizing the Equivalent Consumption Minimization Strategy (ECMS) for the control of hybrid powertrains.

Key findings include:

- The BEV simulation demonstrated the viability and performance benefits of fully electric propulsion.
- The MPC-based control strategy for HEVs improved fuel efficiency and maintained battery state-of-charge within desired limits by predicting future system behavior.
- ECMS provided a more computationally efficient alternative, achieving near-optimal energy distribution without requiring future prediction, making it suitable for real-time applications.

Both control approaches showed strengths and limitations, with MPC offering higher accuracy and flexibility at the cost of computation, while ECMS delivered fast and practical solutions with simplified assumptions.

Future work can explore adaptive MPC or ECMS methods, integration with real-time traffic data, and expansion to plug-in or full electric hybrid systems. Additionally, the implementation of these strategies in hardware-in-the-loop (HIL) platforms could validate their performance in real-world applications.

In conclusion, the results confirm that advanced control strategies like MPC and ECMS can significantly enhance the performance of electric and hybrid vehicles, supporting the global shift toward cleaner and more energy-efficient transportation solutions.

References

[1] International Energy Agency, "Electric vehicles," https://www.iea.org/energy-system/transport/electric-vehicles, 2023, accessed: 2025-04-11.

[2] A. Huaman-Rivera, R. Calloquispe-Huallpa, A. C. Luna Hernandez, and A. Irizarry-Rivera, "An overview of electric vehicle load modeling strategies for grid integration studies," *Electronics*, vol. 13, p. 2259, 2024, open Access under CC BY license. [Online]. Available: https://www.mdpi.com/2079-9292/13/12/2259

[3] H. Wang, W. Yang, Y. Chen, and Y. Wang, "Overview of hybrid electric vehicle trend," in *AIP Conference Proceedings*, vol. 1955, no. 1, 2018, p. 040160. [Online]. Available: https://doi.org/10.1063/1.5033824

[4] K. V. Singh, H. O. Bansal, and D. Singh, "A comprehensive review on hybrid electric vehicles: Architectures and components," *Journal of Modern Transportation*, vol. 27, no. 2, pp. 77–107, 2019. [Online]. Available: https://doi.org/10.1007/s40534-019-0184-3

[5] E. Database, "Tesla model y specifications - ev database," 2024, accessed: April 21, 2025. [Online]. Available: https://ev-database.org/car/1743/Tesla-Model-Y

[6] T. Inc., "Tesla model y owner's manual," 2024, accessed: April 22, 2025. [Online]. Available: https://www.tesla.com/ownersmanual/modely/en_us/GUID-F617DA3E-11C1-4FBA-98A7-A9C3828E3536.html

[7] International Energy Agency, "Global EV outlook 2023: Catching up with climate ambitions," International Energy Agency (IEA), Tech. Rep., 2023. [Online]. Available: https://www.iea.org/reports/global-ev-outlook-2023

[8] S. Z. Rajper and J. Albrecht, "Prospects of electric vehicles in the developing countries: A literature review," *Sustainability*, vol. 12, no. 5, p. 1906, Mar. 2020.

[9] A. A. Pesaran, “Lithium-ion battery technologies for electric vehicles: Progress and challenges,” *IEEE Electrification Magazine*, vol. 11, no. 2, pp. 35–43, 2023. [Online]. Available: https://norbert.idv.hk/Files_Subjects/EV/Lithium-Ion_Battery_Technologies_for_Electric_Vehicles_Progress_and_challenges.pdf

[10] P. Kumar and S. Majhi, “Introduction to hybrid and electric vehicles,” *National Programme on Technology Enhanced Learning (NPTEL)*, 2014, accessed: Apr. 10, 2025. [Online]. Available: https://nptel.ac.in/courses/108103009

[11] B. Shi, A. I. Ramones, Y. Liu, H. Wang, Y. Li, S. Pischinger, and J. Andert, “A review of silicon carbide mosfets in electrified vehicles: Application, challenges, and future development,” *IET Power Electronics*, vol. 16, no. 6, pp. 985–999, 2023, accessed: 2025-04-13. [Online]. Available: https://ietresearch.onlinelibrary.wiley.com/doi/10.1049/pel2.12524

[12] B. Zhang, F. Xu, and T. Shen, “A real-time energy management strategy for parallel hevs with mpc,” in *2019 IEEE Vehicle Power and Propulsion Conference (VPPC)*. IEEE, 2019, pp. 1–5.

[13] W. Fan, B. Liu, J. Tang, and D. Zhong, “Study on energy management strategy for a p2 diesel hev considering low temperature environment,” https://ssrn.com/abstract=5073757, 2024, available at SSRN 5073757.

[14] W. C. Wilberforce, “Electric vehicles market intelligence report,” Greencape, Tech. Rep., 2021, accessed: 2025-04-11. [Online]. Available: https://greencape.co.za/wp-content/uploads/2022/10/EV_MIR_9_4_21-3.pdf

[15] BloombergNEF. (2024) Lithium-ion battery pack prices see largest drop since 2017, falling to $115 per kilowatt-hour. BloombergNEF. Accessed: 2025-04-12. [Online]. Available: https://about.bnef.com/blog/lithium-ion-battery-pack-prices-see-largest-drop-since-2017-falling-to-115-per-kilowatt-hour/

[16] UFine Battery, “What is the energy density of a lithium-ion battery?” https://www.ufinebattery.com/blog/what-is-the-energy-density-of-a-lithium-ion-battery/, 2025, accessed: Apr. 10, 2025.

[17] B. Halvorson. (2020, September) Tesla battery day: Automaker aims to make breakthrough cell at half the cost, could supply other automakers. Accessed: 2025-04-12. [Online]. Available: https://www.greencarreports.com/news/1129700_tesla-claims-breakthrough-cell-to-be-half-the-cost-could-supply-other-automakers

[18] K. Jennings. (2022, February 25) New 800-volt fast charging systems. Accessed: 2025-04-13. [Online]. Available: https://www.greencars.com/news/new-800-volt-fast-charging-systems

[19] B. Electric, "Types of motors in electric vehicles," 2024, accessed: Apr 16, 2025. [Online]. Available: https://bilitielectric.com/blog/types-of-motors-in-electric-vehicles/

[20] E. Technologies. (2023, April) Ev power electronics explained. Accessed: 2025-04-17. [Online]. Available: https://www.exro.com/industry-insights/ev-power-electronics-explained

[21] Charged Future, "Ev charging vs. gas refueling," https://www.chargedfuture.com/ev-charging-vs-gas-refueling/, 2024, accessed: Apr. 19, 2025.

[22] P. Asinger. (2024) Understanding lithium-ion battery degradation. Zitara, last updated Dec. 3, 2024. Accessed: Apr. 19, 2025. [Online]. Available: https://www.zitara.com/resources/lithium-ion-battery-degradation

[23] International Energy Agency. (2023) Global EV outlook 2023: Trends in charging infrastructure. Accessed: Apr. 19, 2025. [Online]. Available: https://www.iea.org/reports/global-ev-outlook-2023/trends-in-charging-infrastructure

[24] A. F. Rochas. (2025, Mar.) Us grids must harness electric vehicle growth to tackle load risks. Accessed: 2025-04-19. [Online]. Available: https://www.reuters.com/business/energy/us-grids-must-harness-electric-vehicle-growth-tackle-load-risks-2025-03-18/

[25] J. O'Dell. (2023, Oct.) Big gap remains in average price of electric car vs. gas car. Edmunds. Accessed: 2025-04-19. [Online]. Available: https://www.edmunds.com/car-buying/average-price-electric-car-vs-gas-car.html

[26] N. Carey. (2024, Sep.) Mercedes teams up with factorial to develop solid-state batteries. Reuters. Accessed: 2025-04-

20. [Online]. Available: https://www.reuters.com/business/autos-transportation/mercedes-teams-up-with-factorial-develop-solid-state-batteries-2024-09-10/

[27] Spherical Insights LLP. (2024, May) Global vehicle-to-grid (v2g) technology market size to worth usd 123.5 billion by 2033. Spherical Insights LLP. Accessed: 2025-04-20. [Online]. Available: https://www.globenewswire.com/news-release/2024/05/16/2883651/0/en/Global-Vehicle-to-Grid-V2G

[28] International Renewable Energy Agency (IRENA), "Smart electrification with renewables: Driving the transformation of energy services," International Renewable Energy Agency, Abu Dhabi, United Arab Emirates, Tech. Rep., 2022, accessed: 2025-04-20. [Online]. Available: https://www.irena.org/publications/2022/Jul/Smart-Electrification-with-Renewables

[29] L. Wang, M. Li, Y. Wang, and Z. Chen, "Energy management strategy and optimal sizing for hybrid energy storage systems using an evolutionary algorithm," *IEEE Transactions on Intelligent Transportation Systems*, vol. 23, no. 9, pp. 14 283–14 293, 2021.

[30] J. Tang, L. Guo, B. Gao, Q. Liu, S. Yu, and H. Chen, "Energy management of a parallel hybrid electric vehicle with cvt using model predictive control," in *2016 35th Chinese Control Conference (CCC)*. IEEE, 2016, pp. 4396–4401.

[31] United Nations Economic Commission for Europe, "Regulation no. 101 of the economic commission for europe of the united nations (un/ece)," 2012, accessed: 2025-05-11. [Online]. Available: https://eur-lex.europa.eu/eli/reg/2012/101(2)/oj/eng

[32] B. Zhou, "Hybrid electric vehicle energy management strategy with consideration of battery aging," Ph.D. dissertation, Michigan Technological University, 2020.